Cell and Tissue Research (2019) 375:507–529
https://doi.org/10.1007/s00441-018-2917-8

REGULAR ARTICLE

The subcommissural organ and the Reissner fiber: old friends revisited

Rosa I. Muñoz[1] · Thilo Kähne[2] · Hernán Herrera[1] · Sara Rodríguez[1] · Ma. Montserrat Guerra[1] · Karin Vío[1] · René Hennig[3,4] · Erdmann Rapp[3,4] · Esteban Rodríguez[1]

Received: 1 June 2018 / Accepted: 17 July 2018 / Published online: 26 September 2018

Abstract

The subcommissural organ (SCO) is an ancient and conserved brain gland secreting into cerebrospinal fluid (CSF) glycoproteins that form the Reissner fiber (RF). The present investigation was designed to further investigate the dynamic of the biosynthetic process of RF glycoproteins prior and after their release into the CSF, to identify the RF proteome and *N*-glycome and to clarify the mechanism of assembly of RF glycoproteins. Various methodological approaches were used: biosynthetic labelling injecting ^{35}S-cysteine and ^{3}H-galactose into the CSF, injection of antibodies against galectin-1 into the cerebrospinal fluid, light and electron microscopical methods; isolated bovine RF was used for proteome analyses by mass spectrometry and glycome analysis by xCGE-LIF. The biosynthetic labelling study further supported that a small pool of SCO-spondin molecules rapidly enter the secretory pathways after its synthesis, while most of the SCO-spondin molecules are stored in the rough endoplasmic reticulum for hours or days before entering the secretory pathway and being released to assemble into RF. The proteomic analysis of RF revealed clusterin and galectin-1 as partners of SCO-spondin; the in vivo use of anti-galectin-1 showed that this lectin is essential for the assembly of RF. Galectin-1 is not secreted by the SCO but evidence was obtained that it would be secreted by multiciliated ependymal cells lying close to the SCO. Further, a surprising variety and complexity of glycan structures were identified in the RF *N*-glycome that further expands the potential functions of RF to a level not previously envisaged. A model of the macromolecular organization of Reissner fiber is proposed.

Keywords Subcommissural organ · SCO-spondin · Galectin-1 · Clusterin · Reissner fiber assembly · Biosynthetic labelling · Mass spectrometry · Immunoblockage · Immunocytochemistry · *N*-glycome

Dedicated to three pioneers of subcommissural organ research, the late Professors Ragnar Olsson (Department of Zoology, University of Stockholm, Sweden), Andreas Oksche (Institut für Anatomie und Zytobiologie, Justus-Liebig-Universität, Giessen, Germany) and Günther Sterba (Abt. Zellbiologie und Regulation, Universität Leipzig, Germany).

Dr. Hernán Herrera has passed away. He contributed substantially to the biosynthetic labelling study.

✉ Esteban Rodríguez
erodrigu@uach.cl

[1] Instituto de Anatomía, Histología y Patología, Facultad de Medicina, Universidad Austral de Chile, Valdivia, Chile

[2] Institute of Experimental Internal Medicine, Otto-von-Guericke University Magdeburg, Leipziger Str. 44, 39120 Magdeburg, Germany

[3] Max Planck Institute for Dynamics of Complex Technical Systems, Sandtorstr. 1, 39106 Magdeburg, Germany

[4] glyXera GmbH, Leipziger Str. 44 - ZENIT Building (House 65), 39120 Magdeburg, Germany

Introduction

The subcommissural organ (SCO) is an ancient and conserved brain gland present throughout the vertebrate phylum. It is located at the roof of the third ventricle, at the entrance of the aqueduct of Sylvius (SA). SCO cells continuously secrete high molecular mass glycoproteins into the cerebrospinal fluid (CSF) where at least some of them condense to form a filamentous structure known as Reissner fiber (RF; Nicholls 1913; Sterba 1969; Rodríguez et al. 1992, 1998). RF is a dynamic structure that continuously grows caudally by the addition of newly released molecules to its cephalic end. It extends through the SA, the fourth ventricle and the central canal of the spinal cord to reach the *massa caudalis* located at the end of the central canal. When arriving at the *massa caudalis*, RF glycoproteins undergo a chemical modification, disassembly and passage into neighboring vessels (Olsson 1955, 1958; Peruzzo et al. 1987; Rodríguez et al. 1998).

Despite more than a century of research on the SCO-RF complex, some relevant questions, such as the full molecular composition of RF or the mechanism leading to the aggregation of its proteins, are yet unsolved. This information seems essential when interpreting the potential role of the SCO-RF complex in brain physiology, especially when increasing evidence has shown that RF is indispensable to maintain the patency and the normal flow of CSF through the SA (Cifuentes et al. 1994; Ortloff et al. 2013; Vío et al. 2000). Further, RF has the capacity to selectively bind and transport away amines, thus contributing to the clearance of these compounds from the CSF (Rodríguez and Caprile 2001; Caprile et al. 2003; S Rodríguez et al. 1999b).

Antibodies against bovine RF glycoproteins specifically recognize the secretory material present in the SCO of all vertebrate species examined except anthropoid apes and human (Oksche et al. 1993; Rodríguez et al. 1984; Sterba et al. 1982) and in the floor plate (Rodríguez et al. 1996; Yulis et al. 1998). When used for immunoblot analyses of bovine SCO, RF antibodies recognize precursor (540 and 320 kDa) and processed (450 and 190 kDa) forms (Nualart et al. 1991; Nualart and Hein 2001). A high conservation of the sugar moieties has been also revealed using lectins. *N*-linked high-mannose chains are associated with the precursor form of the secretion located in the endoplasmic reticulum of SCO cells; complex-type carbohydrates are associated with the mature forms in RF (Herrera and Rodríguez 1990; Meiniel and Meiniel 1985; Meiniel et al. 1988; Rodríguez et al. 1986, 1990). SCO-spondin has been identified as the major and specific component of the SCO/RF complex in bovine (Gobron et al. 1996, 2000; Nualart et al. 1998).

In chick embryos, there is a 4-day delay between the first signs of secretory activity of the SCO ependymal cells and the first appearance of a RF proper (Schöbitz et al. 1986). In rats, this delay is more pronounced, taking 5 postnatal days for the appearance of polymerized secretory material (RF-like) within the aqueduct and 12 days for the formation of the first RF (Schöbitz et al. 1993). Similar studies in bovine fetuses have shown that visualization of the first RF is delayed by 17 days with respect to the first signs of SCO secretory activity (Meiniel et al. 1990). Thus, during embryonic development of the chick, rat and bovine, the secretory material released by the SCO cells remains soluble in the CSF. This led Schöbitz et al. (1986) to conclude that factors other than the ventricular release of the SCO secretory material are required for the formation of RF.

What are the mechanisms operating so that the CSF soluble SCO secretion, SCO-spondin in particular, starts to become densely packed into the CSF insoluble RF? Olsson (1958) and Oksche (1961) postulated that the hydrodynamic of the CSF flowing through the Sylvius aqueduct plays a role in the aggregation of the proteins forming RF. This hypothesis is supported by the fact that hydrocephalic mice and rats do not form a RF (Irigoin et al. 1990; Ortloff et al. 2013; Wagner et al. 2003). However, the fact that SCO isografted into the rat lateral ventricle does form a RF (S Rodríguez et al. 1999b) supports the view that a CSF compound participates in the assembly of the proteins forming RF and that the rapid and turbulent flow of the CSF entering the cerebral aqueduct does not play a role, as suggested by some authors.

The present investigation was designed to (1) further investigate the dynamic of the biosynthetic process of RF glycoproteins prior and after their release into the CSF, (2) identify the RF proteome and *N*-glycome and (3) clarify the mechanism of assembly of RF glycoproteins.

The biosynthetic labelling study showed that most of the SCO-spondin molecules are stored in RER for hours or days before entering the secretory pathway and being released into the CSF. The proteomic analysis of RF revealed clusterin and galectin-1 (Gal-1) as partners of SCO-spondin; the in vivo use of anti-galectin 1 showed that this lectin is essential for the assembly of RF. Gal-1 is not secreted by the SCO but evidence was obtained that it would be secreted by multiciliated ependymal cells lying close to the SCO. Further, a surprisingly large variety and complexity of glycan structures was identified in the RF *N*-glycome; this further expands the potential functions of RF to a level not previously envisaged.

Material and methods

Animals

Sprague-Dawley rats were handled and cared for according to the principles approved by the National Research Council of Chile (Conicyt) and following the regulations approved by the council of the American Physiological Society. Rats were maintained under a 12-h light/12-h dark cycle (light from 8:00 a.m. to 8:00 p.m.) and constant temperature (22 °C), with water and food provided ad libitum.

Biosynthetic labelling and autoradiography

Sixty-four male Sprague-Dawley rats, about 2 months old, were weighed and anesthetized by an intraperitoneal injection of ketamine (60 mg/kg body weight) and Pacifor (1 mg/kg body weight) and positioned on a stereotaxic apparatus. The skin over the skull was incised and a small hole was made in the skull above the target using a micro drill. A 27-gauge cannula was inserted into the lateral ventricle; the stereotactic coordinates were 1.0 mm rostral from the bregma, 1.0 mm lateral from the sagittal suture and 4.0 mm ventral from the dura for injection into the lateral ventricle. The implanted cannula was connected through a polythene tube (0.4 mm I.D.; 0.8 mm O.D.), to an infusion pump with a delivering rate of 1 μl/min. The 64 experimental animals were divided into

two groups, the former receiving 50 μCi of ^{35}S-labeled cysteine (Amersham Radiochemical Centre, specific activity 61.2 mCi/mmol) ($n = 32$) and the later receiving 1.0 μCi of D- [6- ^{3}H]galactose (Amersham Radiochemical Centre; specific activity 26 Ci/mmol) ($n = 32$). After perfusion, the needle was left in place for 10 min prior to withdrawal. Animals were sacrificed at different times after injection, 10, 20 and 30 min; 1, 2 and 3 h; and 1 and 4 days. The central nervous system of rats was fixed by vascular perfusion with Bouin fluid. Then, the brains and the spinal cords were dissected out and immersed in fresh fixative for 2 days. Embedding was in paraffin. Serial sagittal or transverse sections (5 μm thick) were obtained and used for immunocytochemistry (see above) or autoradiography. The method for autoradiography has been described in detail in previous publications (Ermisch 1973; Attila and Talanti 1973; Sterba et al. 1967b). It involves the application to the sections of a thin uniform layer of Ilford L-4 Nuclear liquid emulsion (Polysciences, Inc). Sections were revealed after 4 weeks at − 70 °C using Kodak developer D-19b and F-5 as fixer. Adjacent 5-μm-thick sections were immunostained with the antiserum AFRU (see below).

Injection of antibodies against Gal-1 into the cerebrospinal fluid

Two female Sprague-Dawley rats, about 2 months old, were weighed and anesthetized by an intraperitoneal injection of ketamine (60 mg/kg body weight) and Paciform (1 mg/kg body weight) and positioned on a stereotaxic apparatus. Animals received 20 μg of anti-galectin-1 rabbit polyclonal antibody (Chemicon, Millipore) following the same procedure that was used for ^{35}S-cysteine. After perfusion, the needle was left in place for 10 min prior to withdrawal. Animals were sacrificed 3 h after injection. The central nervous system of rats was fixed by vascular perfusion with Bouin fluid. Then, the brains and the spinal cords were dissected out and immersed in fresh fixative for 2 days. Embedding was in paraffin. Serial sagittal or transverse sections (5 μm thick) were obtained and used for an *incomplete immunostaining procedure*, omitting the incubation with anti-galectin (see below). This procedure demonstrates exclusively the injected antibody. Adjacent 5-μm-thick sections were immunostained with the antiserum AFRU (see below).

Reissner fiber collection

Reissner fiber was obtained by perfusing the central canal of the bovine spinal cord with artificial CSF (Wolf and Sterb 1972; Rodríguez et al. 1984a). Briefly, the spinal cord of each cow was cut into segments of about 20 cm; they were held vertically and a cannula connected to a perfusion pump was inserted into the central canal to perfuse the RF. At the distal end of the perfused segment, the 20 cm of RF were collected as a small tangled ball. The perfused RF was fixed by immersion in a triple aldehyde fixative mixture containing 4% paraformaldehyde, 2% glutaraldehyde, and 2% acrolein and processed for transmission electron microscopy (see below), or was fixed by immersion in 4% paraformaldehyde and processed for whole mount immunofluorescence with AFRU and galectin-1 (see below). The RF glycoproteins were solubilized in 50 mM ammonium bicarbonate as previously described (Nualart et al. 1991) for biochemical analysis. For proteome and glycome analysis, native non-fixed RF was used.

Immunoblot analyses

Samples (15 μl) of solubilized isolated native bovine Reissner fiber (RF) were subjected to SDS-PAGE using a 5–15% polyacrylamide linear gradient. Proteins were transferred to nitrocellulose membranes (Towbin et al. 1979). To block nonspecific binding, blots were saturated with 5% non-fat milk in 0.1 M PBS containing 0.15 mM NaCl and 0.1% Tween-20 (Sigma, Madrid, Spain), for 90 min. Anti-galectin-1 raised in rabbits (Chemicon, Millipore) was used as primary antiserum, at a 1:3500 dilution, for 2 h. Anti-rabbit IgG-HRP (Pierce, Rockford, IL, USA) was used at 1:25,000 dilution, for 1.5 h. Incubations were at room temperature and in darkness. Immunoreactive polypeptides were detected by using an enhanced chemiluminescence (ECL) system (Super Signal, Pierce, Rockford, IL, USA) as instructed by the manufacturer. Molecular weight standards in the range of 10–250 kDa were used (Bio-Rad, Hercules, CA, USA). Control blots were processed as above without the primary antibody.

Reissner fiber extracts and nanoLC-ESI-MS/MS analyses

Isolated bovine Reissner fiber was solubilized in 8 M Guanidinium hydrochloride forced by sonication on ice for 1 h. Subsequently, the sample was diluted with the tenfold volume of 50 mM NH_4HCO_3. Cystein residues of proteins were reduced by addition of 1 mM dithiothreitol for 1 h and further carbamidomethylated by adding 5 mM iodineacetamide for 1 h at room temperature. An aliquot of the sample was subjected to deglycosylation by addition of 0.5 U PNGase F (Sigma) at 37 °C for 16 h. All samples were subjected to limited proteolytic digestion by adding 0.5 μg Trypsin gold (Promega) and incubation at 37 °C overnight. After drying them down in a vacuum centrifuge, peptides were re-dissolved in 5 μl 0.1% trifluoroacetic acid (TFA) and purified on a 250-nl reversed-phase (C18, Poros R2)-nanocolumn. Peptides were eluted in 7 μl 70% (*v*/*v*) acetonitrile (ACN) and subsequently dried in a vacuum centrifuge.

NanoLC-MS/MS analysis was performed on a hybrid dual-pressure linear ion trap/orbitrap mass spectrometer (LTQ Orbitrap Velos Pro, Thermo Scientific, San Jose, USA)

equipped with an U3000 nano-flow HPLC (Thermo Scientific, San Jose, CA) as described earlier (Kähne et al. 2006). The procedure in brief: peptide samples were adjusted to 10 μl 2% ACN/0.1% TFA and fractionated on a 75 μm (inner diameter), 25 cm PepMap C18-column, packed with 2 μm resin (Dionex, Thermo Scientific). Separation was achieved through applying a gradient from 2 to 35% ACN in 0.1% formic acid over 150 min at a flow rate of 300 nl/min. An Orbitrap full MS scan was followed by up to 15 LTQ MS/MS runs using collision-induced fragmentation (CID) of the most abundantly detected peptide ions. Essential MS settings were as follows: full MS (FTMS; resolution 60,000; m/z range 400–2000); MS/MS (Linear Trap; minimum signal threshold 500; isolation width 2 Da; dynamic exclusion time setting 30 s; singly charged ions were excluded from selection). Normalized collision energy was set to 35% and activation time to 10 ms. Raw data processing, protein identification and assignment of the Orbitrap data were performed by PEAKS Studio 7.0 (Bioinformatics Solutions, Waterloo, Canada). False discovery rate (FDR) was set to < 1%.

Characterization of Reissner fiber proteins *N*-glycosylation

N-glycan structures of Reissner fiber were analyzed by multiplexed capillary gel electrophoresis with laser-induced fluorescence detection (xCGE-LIF), as previously described (Hennig et al. 2016; Ruhaak et al. 2010) with some slight modifications. In CGE, the sample separation takes place in a gel-(organic polymer mixed with aqueous buffer)-filled capillary, along an applied high electric field. The separation is based on differences in the m/z-ratio and the shape of the analyzed molecules. Highly charged molecules with a low mass are migrating faster than those with lower charges and/or higher masses. Additionally, the sieving effect of the gel enhances and refines this separation by the molecular shape (hydrodynamic cross-section) of the analytes. Analytes with a small hydrodynamic cross-section are migrating faster than those with a bigger one.

For xCGE-LIF analysis, *N*-glycans were released from Reissner fiber extract by PNGase F (P7367, Sigma-Aldrich) treatment for 16 h at 37 °C. To make *N*-glycans detectable by LIF, the released *N*-glycans were labeled with the fluorescent dye 8-aminopyrene-1,3,6-trisulfonic acid (APTS, Sigma-Aldrich). Excess of label, salt and other impurities was removed by a post-labelling sample clean-up using glyXbeads™ (glyXera GmbH, Magdeburg, Germany). The purified APTS labeled *N*-glycans were analyzed by xCGE-LIF. The data evaluation was performed using glycoanalysis software (glyXtool™ v5.3.1) and database (glyXbase™) from glyXera. Doing so, the recorded *N*-glycan electropherograms were normalized to an internal standard, resulting in a so-called "*N*-glycan fingerprint" with highly reproducible standardized migration time units (MTU). Subsequently, using glyXtool™ and glyXbase™, a structural assignment of the *N*-glycan peaks was performed. To confirm these assignments, a comprehensive exoglycosidase treatment was conducted, using the enzymes α(2–3) sialidase (GK80020, Prozyme), α(2–3,6,8) sialidase (GK80040, Prozyme), α(1–2) fucosidase (P0724S, New England Biolabs), α(1–3,4) fucosidase (E-F134, QABio), α(1–2,3,4,6) fucosidase (GKX-5006, Prozyme), β(1–3) galactosidase (P0726S, New England Biolabs), β(1–4) galactosidase (P0745S, New England Biolabs), β(1–2,3,4,6)-N-acetylglucosaminidase (P0744S, New England Biolabs) and α(1–2,3,6) mannosidase (GKX-5010, Prozyme). All exoglycosidase digests were carried out at 37 °C and at the reaction conditions recommended by the respective enzyme supplier. Each exoglycosidase enzyme was carefully tested for activity, specificity and possible side activities (data not shown). As a final step, the symbolic representation of *N*-glycans (assigned by glyXbase™ and confirmed by exoglycosidase sequencing) were depicted on each *N*-glycan peak of the *N*-glycan fingerprint. The symbolic representations were drawn with GlycoWorkbench (Ceroni et al. 2008), according to the guideline of the Consortium for Functional Glycomics (Varki et al. 2009).

Light microscopy tissue processing

The subcommissural organs and spinal cord from adult cows were fixed by immersion with Bouin fixative. Embedding was in paraffin. Samples were cut serially at a thickness of 5 μm. Sections were used for immunohistochemistry and immunofluorescence (see below).

Pseudoisocyanine staining

Sections of the adult rat subcommissural organ were studied with N-N′ diethyl pseudoisocyanine chlorhydrate (PIC) stain for the detection of disulfide bonds (Sterba 1964, 1966). A metachromatic stain, tinted red in the monomer state, purplish red as a polymer, PIC present a yellow fluorescence. Following methylation and oxidation, sections were mounted in a glycerol mixture containing para-phenylenediamine (PPD), in order to intensify and extend fluorescence and were studied under an epifluorescence microscope. Pseudoisocyanine sulfatide-micelles have a maximum absorption at 583 nm (maximum absorption of the monomeric dye is at 530 nm).

Immunohistochemistry

Sections from the subcommissural organs and spinal cord from adult cows were processed for immunohistochemistry as described by Sternberger et al. (1970) or the streptavidin-

biotin method (Vectastain kit, VECTOR, SERVA, Heidelberg, Germany), with diaminobenzidine as electron donor. The following primary antibodies were used: (1) AFRU (antisera raised in rabbits against isolated bovine fiber of Reissner dissolved in a medium containing urea; Rodríguez et al. 1984a) was used at a dilution of 1:1000; (2) RAFRU (same as AFRU but raised in rats) antibody was raised in rats against the constitutive glycoproteins of the bovine RF and specifically reacts with the high molecular weight glycoproteins secreted by the SCO into the CSF. RAFRU was used at a dilution of 1:500; (3) anti-caveolin-1 (Santa Cruz Biotechnology) was used at a dilution 1:100; (4) anti-Gal-1 was used at a dilution of 1:500. Antibodies were diluted in a buffer containing 0.1 M Tris buffer, pH 7.8, 0.7% non-gelling seaweed gelatine lambda carrageenan and 0.5% Triton X 100 (Sigma, St. Louis, MO, USA). Incubation was carried out for 18 h at room temperature. Omission of the primary antibody during incubation provided the control for the immunoreaction.

Whole mount immunofluorescence

To stain whole mount, RF was washed with phosphate-buffered saline (PBS) and incubated at room temperature with AFRU (1:1000) or anti-galectin 1 (1:500) antibodies (raised in rabbits) for 48 h. After being washed in PBS, appropriate secondary antibodies conjugated with Alexa Fluor 594 (1:500; Invitrogen, Carlsbad, CA) were used. Omission of the primary antibody during incubation provided the control for the immunoreactions. Immunostained RF was studied under an epifluorescence microscope using the multidimensional acquisition software AxioVision Rel (version 4.6) of Zeiss (Aalen, Germany).

Double immunofluorescence and confocal microscopy

For double immunofluorescence, sections were incubated overnight at room temperature with primary antibodies (raised in rats or rabbits) for 18 h. The following pairs of antibodies were used: (1) AFRU (dilution 1:1000)/anti-β-tubulin IV (monoclonal antibody, dilution 1:100; AbCam,UK); (2) anti-S100β (rabbit polyclonal antibody, dilution 1:100, AbCam)/RAFRU (dilution 1:500). After being washed in Tris buffer, pH 7.8, sections were incubated with appropriate secondary antibodies conjugated with Alexa Fluor 488 or 594 (1:500; Invitrogen, Carlsbad, CA). Antibodies were diluted in a buffer containing 0.1 mol/L Tris buffer, pH 7.8, 0.7% non-gelling seaweed gelatin, lambda carrageenan and 0.5% Triton X-100 (Sigma). Omission of the primary antibody during incubation provided the control for the immunoreactions. Slides were studied under an epifluorescence microscope using the multidimensional acquisition software AxioVision Rel (version 4.6) of Zeiss (Aalen, Germany) or by confocal microscopy (Zeiss LSM700) with the acquisition software Zen 2012.

Transmission electron microscopy tissue processing

The bovine perfused RF and the brain tissue from rats were prepared as for light microscopy (see above) except that a triple aldehyde fixative mixture containing 4% paraformaldehyde, 2% glutaraldehyde and 2% acrolein in 0.2 M phosphate buffer, pH 7.4, was used (Rodríguez 1969). A sagittal cut through the lateral region of the skull was performed to expose the brain tissue; fixative was gently subperfused into the exposed brain cavities using a microliter syringe. The head was immersed in the same fixative for 20 min and the brain was dissected out and immersed again in the fixative for 2 h. The bovine perfused RF and blocks of tissue containing the SCO and rostral third of the SA were obtained and fixed in 1% OsO_4 in 0.1 M phosphate buffer, pH 7.4, for 2 h at 4 °C. Embedding was in Epon. Sections were contrasted with lead citrate and uranyl acetate and analyzed under a Hitachi H-700 electron microscope.

Transmission electron microscopy immunocytochemistry

The SCO of rats was fixed by vascular perfusion with a mixture containing 2% paraformaldehyde, 0.5% glutaraldehyde and 15% saturated picric acid solution in 0.1 M phosphate buffer, pH 6.0. The blocks of tissue containing the SCO were postfixed with 0.25% OsS4. Embedding was in butyl-methyl methacrylate (Rodríguez et al. 1984b). Ultrathin sections mounted on nickel grids were processed for the immunoperoxidase-silver methenamine method (Rodríguez et al. 1984b). AFRU was used as primary antibody, at a dilution of 1:2000 for 1 h.

Results

The cells of the SCO show a clear zonation, with the different compartments of the secretory pathways localized in discrete regions of the cytoplasm

The SCO ependymocytes are tall cylindrical cells, about 80 to 100 μm high. The use of (i) a fluorescence dye, pseudoisocyanin, specific for disulphide bonds (Fig. 1c), (ii) immunofluorescence using antibodies specific for Reissner fiber glycoproteins (AFRU, anti-RF proteins generated in rabbits; RAFRU, anti-RF proteins generated in rats) and other cell components (Fig. 1a, b), (iii) transmission electron microscopy (Fig. 1f, g) and ultrastructural immunocytochemistry

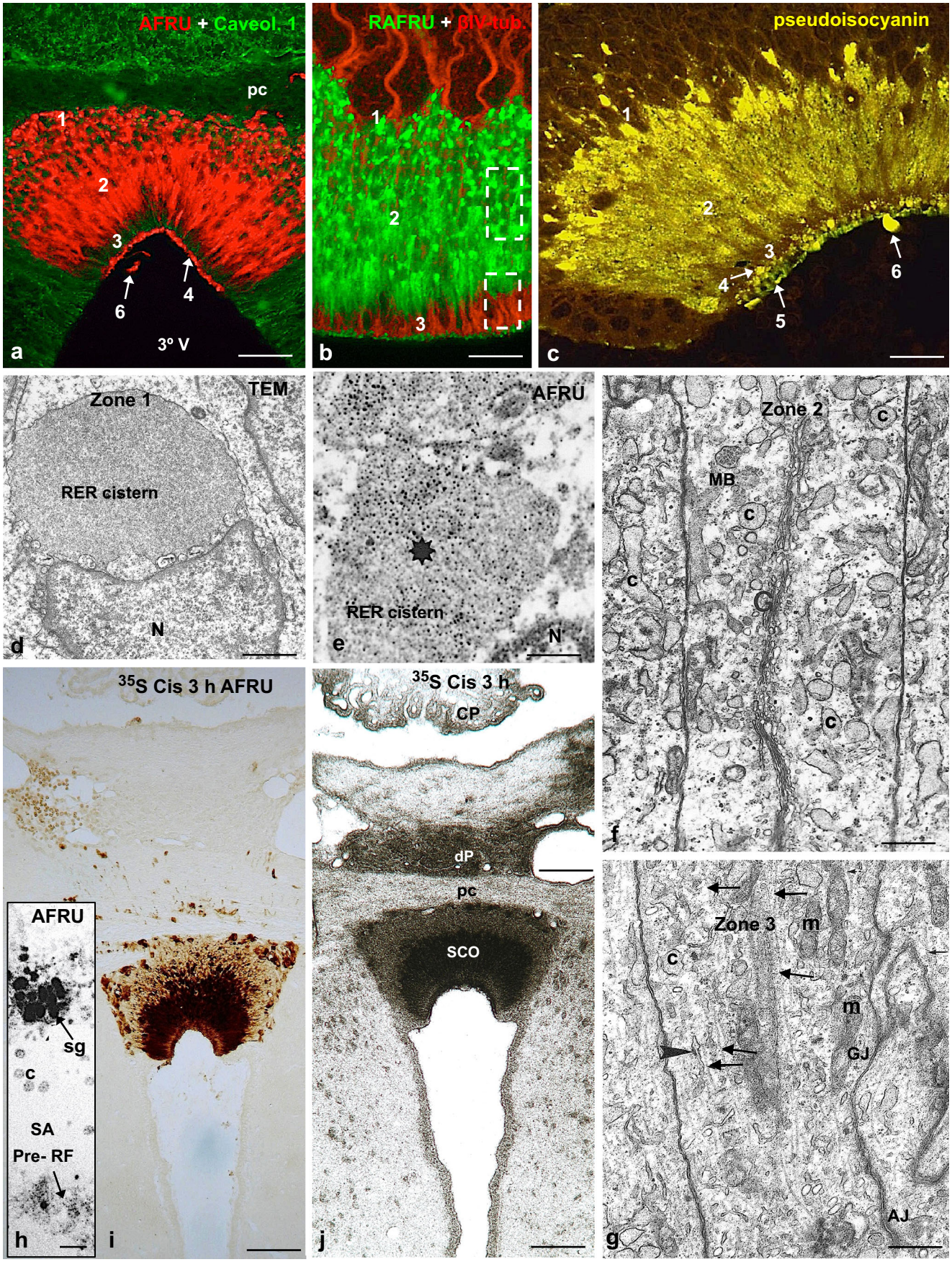
AFRU + Caveol. 1
pc
1
2
3
4
6
3° V
a
RAFRU + βIV-tub.
1
2
3
b
pseudoisocyanin
1
2
3
4
5
6
c
Zone 1
TEM
RER cistern
N
d
AFRU
RER cistern
N
e
Zone 2
c
MB
c
c
c
c
f
35S Cis 3 h AFRU
AFRU
sg
c
SA
Pre- RF
h
i
35S Cis 3 h
CP
dP
pc
SCO
j
Zone 3
m
c
m
GJ
AJ
g

◀ **Fig. 1** The subcommissural organ (SCO)-Reissner Fiber complex of the rat. **a** Double labelling with AFRU (*red*) and anti-caveolin 1 (*green*). The ependymal cells of the SCO are bipolar, with an apical pole contacting the ventricular CSF and a basal process projecting to local capillaries and to the subarachnoid space. Secretory ependymocytes of the SCO present a clear zonation: 1) subnuclear region, 2) supranuclear and intermediate regions, 3) subapical region, 4) apical cell pole, 5) pre-RF and, 6) RF proper. (*PC*, posterior commissure). **b** Double-immunolabeling with AFRU (*green*) and anti-βIV-tubulin (*red*) shows the subapical zone (3) devoid of AFRU+ material and containing microtubules (*red*). The two rectangles frame areas similar to those shown in **f** and **g**. **c** Pseudoisocyanin staining showing the zonation of ependymal cells of the SCO. The secretory material upon release condenses, first as a film on the surface of the organ (pre-RF) (5) and, after further packaging, into Reissner fiber (6). **d** Ultrastructure of the subnuclear zone containing a large rough endoplasmic reticulum (RER) cistern filled with a filamentous material.; *N* cell nucleus. **e** The secretory material stored in the RER cisternae reacts with AFRU (*black star*). **f** Ultrastructure of the supranuclear cytoplasm (*zone 2*; see upper rectangle in **b**) containing the Golgi apparatus (*G*) and numerous dilated small RER cisternae (*c*). *MB* multivesicular body. **g** Ultrastructure of the subapical cytoplasm (*zone 3*; see lower rectangle in **b**) containing a few RER cisternae (*c*), smooth endoplasmic reticulum (*arrowhead*), mitochondria (*m*) and numerous microtubules (*arrows*). *GJ* gap junction, *AJ* adherent junction. **h** Secretory granules (*sg*) packed in the apical cell pole and pre-RF react with AFRU. *c* cilia. **i**, **j** Adjacent sections through the subcommissural organ (*SCO*) immunostained using AFRU (**i**) and processed for radioautography 3 h after ^{35}S-cysteine administration into the CSF (**j**). *PC* posterior commissure, *CP* choroid plexus, *dp* deep pineal. *Bars:* **a** 20 μm; **b** 10 μm; **c** 15 μm; **d** 1 μm; **e** 0.8 μm; **f**, **g** 400 nm; **i**, **j** 40 μm

(Fig. 1e, h) allowed to distinguish six compartments of the secretory pathway. For descriptive purpose, they have been labeled with numbers 1 to 6:

- Compartment 1. Large, dilated cisternae of the rough endoplasmic reticulum (RER), ranging from 3 to 6 μm in diameter, were localized in the basal cell pole, close to the cell nucleus. They were filled with a filamentous material (Fig. 1d) that strongly reacts with AFRU and RAFRU (Fig. 1a–e), and with pseudoisocyanin (Fig. 1c).
- Compartment 2. The cytoplasm extending from the cell nucleus to the apical cell membrane is about 70 μm high. The basal two thirds of this column were occupied by numerous RER cisternae, 0.5 to 1 μm in diameter and by the Golgi apparatus, located in the axis of the column (Fig. 1f). At the light microscopic level, this compartment was strongly reactive with AFRU and RAFRU (Fig. 1a, b) and pseudoisocyanin (Fig. 1c).
- Compartment 3. The subapical region contained numerous microtubules, mitochondria and smooth endoplasmic reticulum and few or none secretory granules (Fig. 1g). This compartment did not react with AFRU or RAFRU, or pseudoisocyanin (Figs. 1a–c) but it did react with anti-βIV-tubulin (Fig. 1b).
- Compartment 4. Secretory granules located at the apical cell pole strongly reacted with AFRU and RAFRU (Fig. 1a–h) and pseudoisocyanin (Fig. 1c).
- Compartments 5 and 6. Upon release, the AFRU+, pseudoisocyanin+ secretory material first aggregated into fibrils that formed a mesh on the surface of the SCO (pre-RF, 5) and, after further packaging, formed Reissner fiber (6) (Fig. 1a–h). Such an aggregation allowed to visualize in tissue sections the secreted proteins.

Biosynthetic labelling reveals unique features of the secretory process in the SCO ependymal cells

The distinct subcellular distribution of the different domains of the secretory pathway allowed to follow the radiolabelled proteins and sugars by using light microscopy radioautography. SCO-spondin, a complex-type, *N*-linked glycoprotein, is the main secretory protein of the SCO forming RF. AFRU selectively reacted with SCO-spondin becoming a good marker of the ependymal and hypendymal secretory cells of the SCO (see below). The biosynthesis of SCO-spondin was tracked by using ^{35}S-cysteine to label the protein and ^{3}H-galactose to label the sugar moiety. Both radioactive compounds were administered into the ventricular CSF of adult rats and the brain was processed at different time intervals after the injection. The combined use in adjacent sections of radioautography and immunocytochemistry for RF glycoproteins allowed to establish the co-existence within the same domains of the secretory pathway of the immunoreactive secretory material and both labels. The progressive appearance and disappearance of both labels along the secretory pathway and their presence in pre-RF and RF, indicated that both radioactive compounds had been incorporated into the newly synthetized secretory glycoproteins.

^{35}S-cysteine labelling Twenty minutes after its injection into the CSF, ^{35}S-cysteine was detected in compartments 2 and 4 but was not yet present in the secreted material (Fig. 2a, b). One hour postinjection, hypendymal cells and compartments 2 and 4 of the ependymal cells were strongly labeled; some label was found in pre-RF (Fig. 2c). Two and 3 h post-administration of the radiolabel, all six compartments of the secretory pathway of the ependymocytes, as well the hypendymal cells, were strongly labeled (Fig. 2d, e). One and 2 days after the ^{35}S-cysteine injection, the secretory pathway, pre-RF and RF in particular, continued to be strongly radioactive (Fig. 2f). Hypendymal cells were weakly labeled. At the fourth day, hypendymal cells were not labeled, the ependymal cells of the SCO had little label but the RF running along the Sylvius aqueduct and fourth ventricle was distinctly labeled (Fig. 2g–j).

^{3}H-galactose labelling Hypendymal cells and compartments 2 and 4 of the ependymal cells were labeled 1 h after the

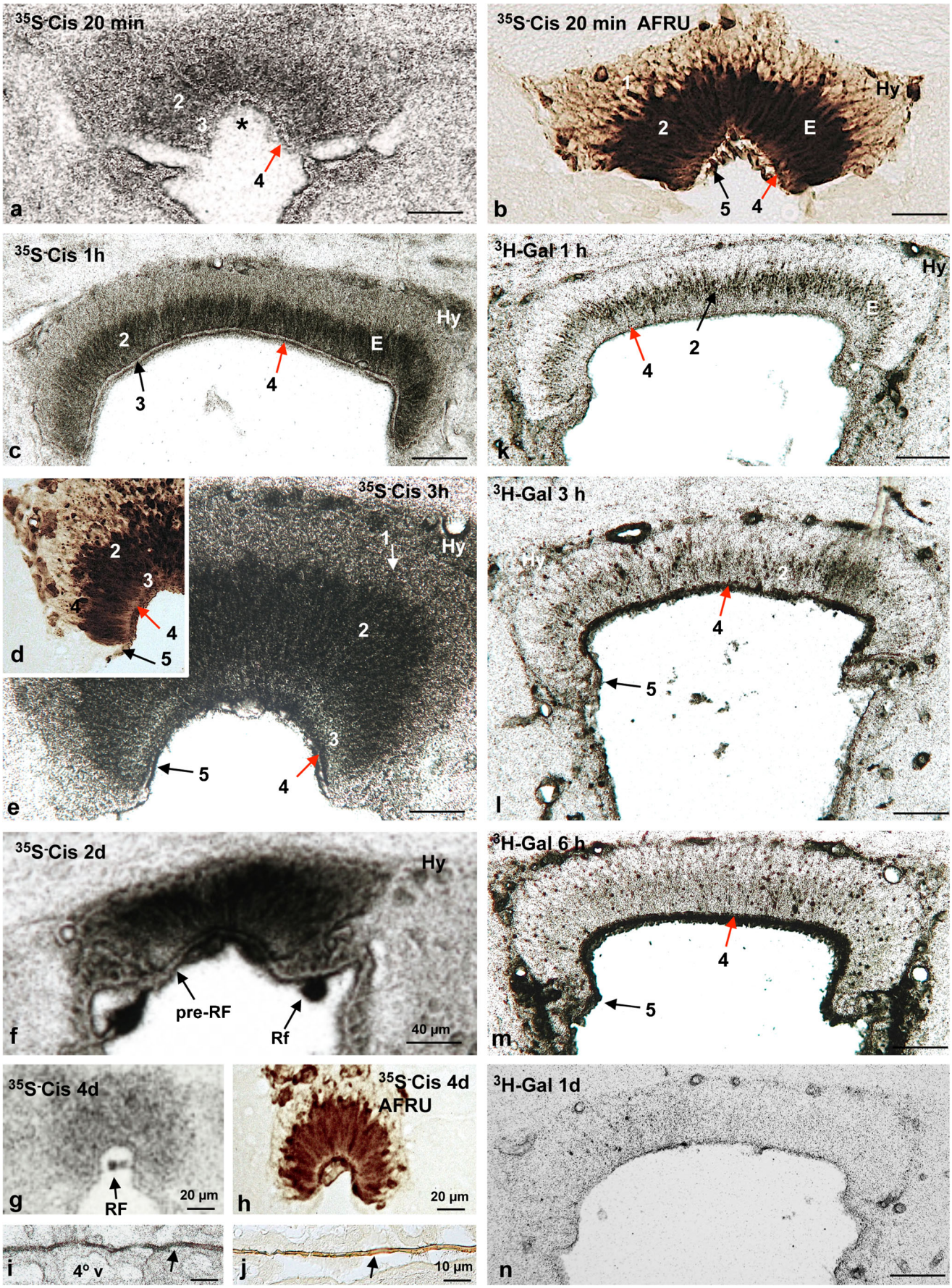
35S-Cis 20 min
2
3
*
4
a
35S-Cis 20 min AFRU
1
Hy
2
E
5
4
b
35S-Cis 1h
Hy
2
E
3
4
c
3H-Gal 1 h
Hy
E
2
4
k
2
3
4
4
5
d
35S-Cis 3h
1
Hy
2
3
5
4
e
3H-Gal 3 h
Hy
2
4
5
l
35S-Cis 2d
Hy
pre-RF
Rf
40 µm
f
3H-Gal 6 h
4
5
m
35S-Cis 4d
RF
20 µm
g
35S-Cis 4d
AFRU
20 µm
h
3H-Gal 1d
n
i
4° v
j
10 µm

◀ **Fig. 2** Biosynthetic labelling of the secretory pathway of SCO-compounds using ^{35}S-cysteine and ^{3}H-galactose. **a, b** Adjacent sections through the subcommissural organ processed for radioautography 20 min after ^{35}S-cysteine administration into the CSF (**a**) and immunostained using AFRU (**b**). AFRU reacts with the RF proteins present in all compartments of the secretory pathways of ependymocytes (*E*, *1–5*) and hypendymal cells (*Hy*) while labeled cysteine is seen only in compartments 2 and 4 of ependymocytes; the AFRU+ pre-RF (*5* in **b**) is not yet radiolabelled (*asterisk* in **a**). **c** Radioautography 1 h after ^{35}S-cysteine administration into the CSF. Zones 2 and 4 of the SCO ependyma (*E*) and hypendymal cells (*Hy*) are labeled. **d**, **e** Adjacent sections through the subcommissural organ immunostained using AFRU (**d**) and processed for radioautography 3 h after ^{35}S-cysteine administration into the CSF (**e**). All compartments of the secretory pathway, including pre-RF (*5*), are labeled. **f** Radioautography 2 days after ^{35}S-cysteine administration into the CSF. The hypendymal cells (*Hy*), the ependymocytes and the released material forming pre-RR and Riessner fibrils (*Rf*) are all strongly labeled. **g**, **h** Adjacent sections through the subcommissural organ processed for radioautography 4 days after ^{35}S-cysteine administration into the CSF (**g**) and immunostained using AFRU (**h**). The ependymocytes and Reissner fiber (RF) display a weak labelling. **i** Four days after ^{35}S-cysteine administration into the CSF Reissner fiber (RF) present in the fourth ventricle (4° v) is radiolabelled throughout. **j** Reissner fiber immunostained with AFRU (*arrow*). **k–n** Frontal sections through the subcommissural organ at different time intervals after the administration of ^{3}H-galactose into the CSF. 1 h after the injection (**k**) compartments 2 and 4 of ependymocytes (*2, 4*) and hypendymal cells (*Hy*) are labeled; 3 h postinjections (**l**), the apical cell pole (*4*) and released material (*5*) are strongly radioactive; 6 h after the injection (**m**), compartment 2 (*2*) is devoid of label while compartments 4 and 5 (*4, 5*) are strongly labeled. One day after ^{3}H-galactose administration (**n**), the SCO is completely depleted of radioactive material. *Bars:* **a**, **b** 40 μm; **c**, **f**, **k**, **l**, **m** 40 μm; **e** 20 μm; **g**, **h** 20 μm; **i**, **j** 10 μm; **n** 67 μm

administration of ^{3}H-galactose (Fig. 2k). Three hours after the injection, compartments 2, 4 and 5 and the hypendymal cells, were strongly labeled (Fig. 2l). At the sixth postinjection hour, compartment 2 was depleted while compartments 4 and 5 continued to be strongly radioactive (Fig. 2m). One day after the injection of ^{3}H-galactose, the SCO was completely devoid of label (Fig. 2n).

The wall of the blood vessels present in the sections through the epithalamus was not labeled by ^{35}S-cysteine in any of the postinjection intervals (Fig. 1i, 2c–f). At variance, the wall of the blood vessels was strongly labeled by ^{3}H-galactose (Fig. 2k–m).

Reissner fiber glycoproteins have a complex pattern of *N*-linked glycans

The glycoproteins extracted from Reissner fiber extract (SCO-spondin, clusterin) (Fig. 3c) showed an enormous variety of different *N*-glycan structures; from simple neutral diantennary *N*-glycans, to highly complex tetraantennary *N*-glycans containing bisecting *N*-acetylglucosamin (GlcNAc), up to three sulfations and/or several sialic acids of the Neu5Gc or Neu5Ac type (Fig. 3a–b', b"). This makes the Reissner fiber *N*-glycosylation one of the most complex in nature.

Galectin 1 (Gal-1) was identified as a new interaction partner of the Reissner fiber glycoproteins (SCO-spondin) (see below). It is known that Gal-1 strongly binds to terminal galactose residues, as well as to α(2–3) linked sialic acids and α(1–2) linked antenna fucose (fucosylated *N*-acetyllactosamine). In contrast, Gal-1 does not bind to terminal α(2–6) linked sialic acids or α(1–3) linked antenna fucose (Camby et al. 2006; Stowell et al. 2006). To identify possible binding partners for Gal-1 at the Reissner fiber glycoproteins, a comprehensive exoglycosidase sequencing of the *N*-glycans was performed. By comparing the α(2–3) sialidase digest to the α(2–3,6,8) sialidase digest, the vast majority of sialic acids could be identified as α(2–3) linked (Fig. 3a, b"). With α(1–2) fucosidase and α(1–3,4) fucosidase treatment of the desialiylated *N*-glycans, the absence of α(1–2) and α(1–3,4) linked antenna fucose was proven (data not shown). The β(1–3) galactosidase and β(1–4) galactosidase treatment confirmed a minor presence of terminal galactoses (data not shown).

The proteomic analysis of Reissner fiber reveals the presence of proteins not previously recorded

In addition to SCO-spondin, the following proteins were identified (Table 1):

- *Gal-1*. With 95% of the peptides covered, the presence of Gal-1 in RF may be considered validated. This was confirmed by the identification of Gal-1 in immunoblot of RF extracts (Fig. 3d) and by the in vitro and in vivo effects on RF of an antibody against Gal-1 (see below). Gal-1 was not detected in the bovine and rat SCO neither by immunocytochemistry or immunoblot.
- *Clusterin*. Clusterin is a 70- to 80-kDa *N*-glycosylated protein. A higher amount of peptides and higher sequence coverage was detected after deglycosylation of RF, indicating that clusterin represents a constituent of RF rather than a protein randomly attached to the fiber.
- *S100β*. The presence of S100β protein in RF extracts detected by mass high-resolution tandem mass spectrometry was confirmed by immunocytochemistry of RF and SCO (see below).
- *Calmodulin.* The high level of peptide coverage indicates that this Ca + binding protein is a component of RF. Confirmation by immunoblotting and immunocytochemistry using anti-calmodulin was not performed.
- *Other proteins*. The spectrometric analysis indicated the probable presence in RF of creatine kinase B-type, tubulin beta and tubulin alpha.

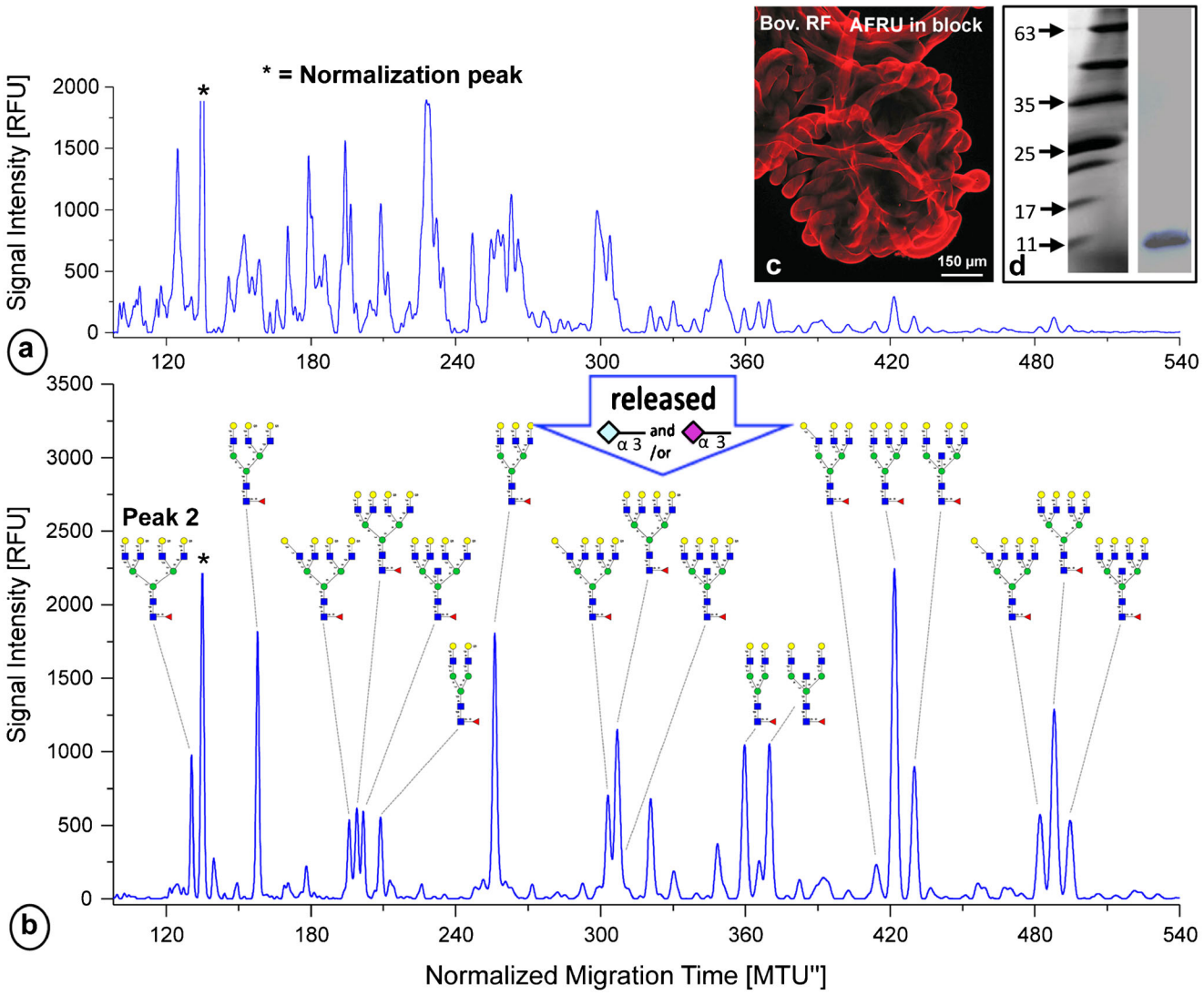
* = Normalization peak
Signal Intensity [RFU]
Bov. RF AFRU in block
150 µm
c
d
63
35
25
17
11
a
b
Peak 2
released
α 3 and /or α 3
Normalized Migration Time [MTU"]

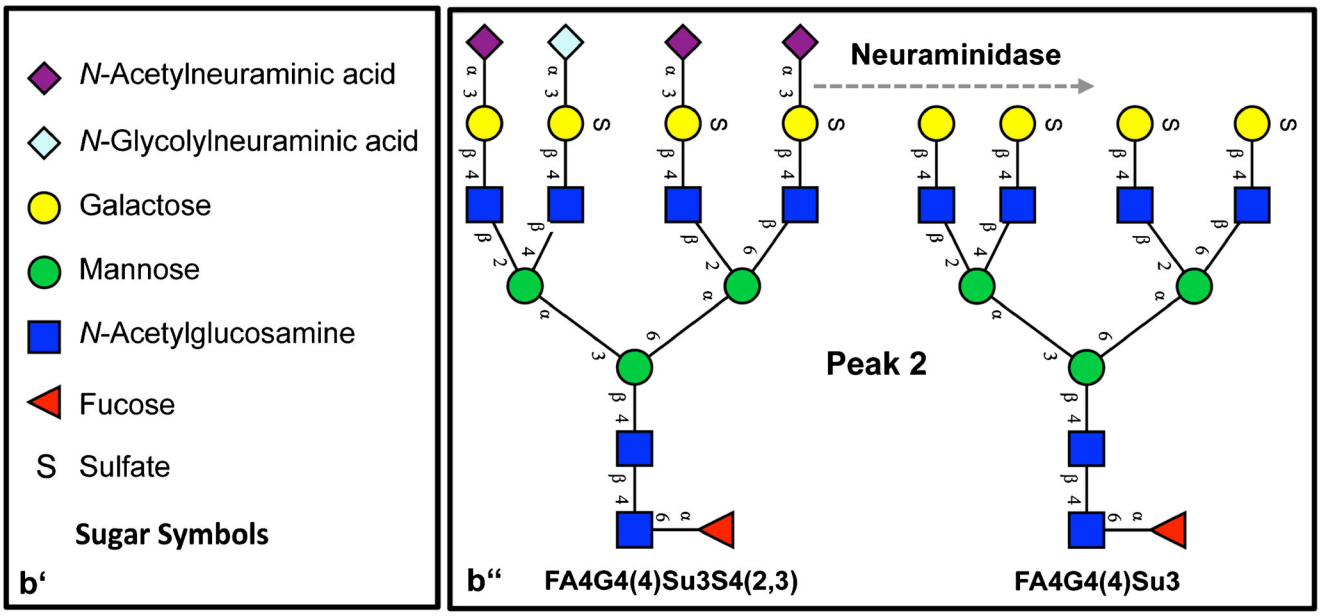
N-Acetylneuraminic acid
N-Glycolylneuraminic acid
Galactose
Mannose
N-Acetylglucosamine
Fucose
S Sulfate
Sugar Symbols
b'
Neuraminidase
Peak 2
b" FA4G4(4)Su3S4(2,3)
FA4G4(4)Su3

◀ **Fig. 3** xCGE-LIF derived fingerprints of the Reissner Fiber *N*-glycosylation pattern. Signal intensity (in relative fluorescence units (RFU)) of APTS labeled *N*-glycans is plotted over their normalized migration time units [MTU"]. **a** Fingerprint of Reissner fiber derived *N*-glycans without enzymatic exoglycosidase treatment. **b** Fingerprint of Reissner fiber derived *N*-glycans after α(2–3) sialidase treatment. The major *N*-glycan structures were annotated via migration time matching with glyXbase™ and confirmed by a series of exoglycosidase digests (see the "Method" section). For the sake of simplification, *N*-glycan structures were only annotated in figure **b**. Each annotated *N*-glycan structure has several sialic acid residues, which create the enormous complexity of the Reissner fiber *N*-glycosylation shown in figure **a**. **b'** Conventional sugar symbols. **b"** *N*-glycan structure of peak 2 shown in **b**, before and after neuraminidase treatment. FA4G4(4)Su3S4(2,3) indicates one fucose (*F*) attached to a four antennary *N*-glycan core (*A4*) with four galactose (*G4*), three sulfate (*Su3*) and four sialic acid (*S4*) residues; *(4)* indicates galactose linked to *N*-acetylglucosamine in β 1–4 position; *(2, 3)* indicates sialic acid linked to galactose in α-2–3 position. **c** Freshly collected bovine Reissner fiber was immunostained in block using AFRU. **d** Immunoblot of RF extract using anti-galectin 1 shows an immunoreactive band of 14 kDa. *Bars:* **c** 150 μm

Macromolecular organization of Reissner fiber

In the bovine SCO, there were three populations of ependymocytes, most cells were AFRU+, S100B-, while small populations were either AFRU−, S100B+ or AFRU+ and S100B+ (Fig. 4a–b'). The AFRU+ Reissner fiber was surrounded by S100B+, AFRU− patches arranged as a beaded ring (Fig. 4c, d, inset).

RF proper is formed by the assembly of bundles of filaments. In fresh, hydrated RF, these filaments were about 2 to 5 μm thick (Fig. 4f–g'). Under in vitro conditions, the fresh RF may spontaneously disassemble with its filaments becoming readily visible (Fig. 4f); an optic dense structure linking transversally the unpacked filaments was observed (Fig. 4f). In tissue sections of dehydrated/embedded RF, the AFRU+ filaments forming RF ranged from 0.5 to 2 μm in thickness and were unevenly distributed throughout the fiber (Fig. 4e).

Transmission electron microscopy of cross-sections of bovine RF revealed that the fiber is essentially formed by microfilament 10–15 nm thick, running longitudinally along the fiber. In the core of RF, such microfilaments are more densely packed than in the cortex (Fig. 5a, b). This spatial organization agrees with the observation that in cross-sections of RF processed for immunocytochemistry, a peripheral ring is more reactive with anti-RF antibodies than the core (Fig. 5a, inset). In sagittal sections of RF, the microfilaments displayed a wavy profile and were packed into bundles, 0.2 to 1 μm thick, running longitudinally. The bundles were linked by horizontally oriented short 7-nm-thick filaments that formed a honeycomb-like structure (Fig. 5c, d). These bundles most likely corresponded to the filaments seen under phase contrast microscopy and by immunofluorescence (see above).

Microvesicles, 100–150 nm in diameter, were present at the border between the core and the cortex of RF (Fig. 5b); some

Table 1 Reissner fiber protein composition resolved by high-resolution tandem mass spectrometry

Description	Accesion	-10lgp	Peptides	Coverage (%)	PNGase
SCO-spondin	P98167	458.98	499	61	–
OS=*Bos taurus* GN=SSPO PE = 2 SV = 2	SSPO_BOVIN	521.86	676	72	+
Galectin-1	P11116	251.53	35	95	–
OS=*Bos taurus* GN = LGALS1 PE = 1 SV = 2	LEG1_BOVIN	264.98	29	95	+
Creatine kinase B-type	Q5EA61	268.79	33	82	–
OS=*Bos taurus* GN=CKB PE = 1 SV = 1	KCRB_BOVIN	295.25	33	86	+
Tubulin beta-2B chain	Q6B856	279.02	43	82	–
OS=*Bos taurus* GN = TUBB2B PE = 1 SV = 2	TBB2B_BOVIN	291.13	35	82	+
Tubulin alpha-1B chain	P81947	257.56	31	70	–
OS=*Bos taurus* PE = 1 SV = 2	TBA1B_ BOVIN	281.54	28	73	+
Protein S100-B	P02638	204.74	19	61	–
OS=*Bos taurus* GN=S100B PE = 1 SV = 2	S100B_BOVIN	216.29	16	65	+
Protein S100-A1	P02638	165.62	6	49	–
OS=*Bos taurus* GN = S100A1 PE = 1 SV = 2	S100B_BOVIN	184.56	7	49	+
Calmodulin	P62157	196.32	15	83	–
OS=*Bos taurus* GN=CALM PE = 1 SV = 2	CALM_BOVIN	217.95	19	99	+
Clusterin	P17697	214.74	15	41	–
OS=*Bos taurus* GN=CLU PE = 1 SV = 1	CLUS_BOVIN	247.59	20	62	+

Isolated bovine Reissner fiber was solubilized in guanidinium hydrochloride and divided into two aliquots. One aliquot was treated with PNGase F to remove the *N*-glycans prior to tryptic digestion and mass spectrometric analysis

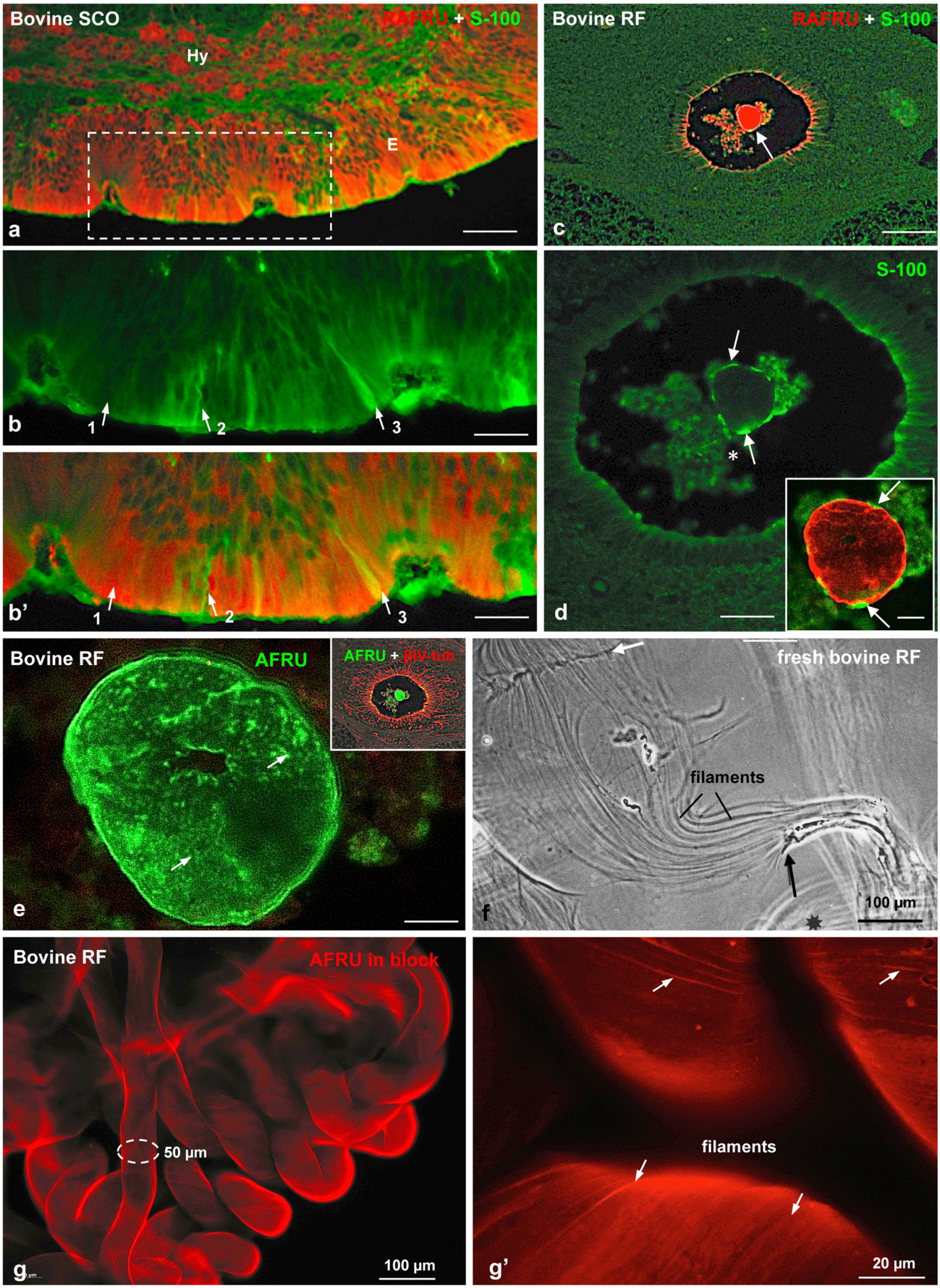
Bovine SCO
RAFRU + S-100
Hy
E
a
Bovine RF
RAFRU + S-100
c
b
1
2
3
b'
S-100
*
d
Bovine RF
AFRU
AFRU + βIV-tub
e
fresh bovine RF
filaments
f
100 µm
Bovine RF
AFRU in block
50 µm
g
100 µm
filaments
g'
20 µm

◀ **Fig. 4** The bovine SCO secretes the S100β factor. **a** Sagittal section of the bovine SCO. Double immunofluorescence with RAFRU (*red*) and S100β (*green*) showing the ependymal (*E*) and hypendymal cells (*Hy*). **b**, **b'** Detailed magnification of area framed in **a**, using the channel for S-100 (**b**) or both channels (**b'**). Three populations of SCO cells can be distinguished: 1. RAFRU+ (*1*, *red*); 2. S100β + (*2*, *green*); 3. RAFRU+ and S100β + (*3*, *yellow*). **c** Frontal section of the bovine spinal cord. Double immunofluorescence with RAFRU (*red*) and S100β (*green*) shows the wall of the central canal and the RF reacting with S100β and RAFRU. **d** and **inset** detailed magnification of previous figure. S100β + patches are located at the periphery of the RF (*arrows*). **e** Magnification of the RF shown in the inset. RF is formed by the assembly of bundles of filaments (*arrows*). **f** Nomarski optic of fresh bovine RF, showing individual filaments becoming visible due to an spontaneous unpackaging of RF starting a given point (*black arrow*). *White arrow* points to a dense structure linking the unpacked filaments. **g**, **g'** In block immunostaining with AFRU. The diameter of the fresh non-dehydrated RF is 50 μm. Individual AFRU+ filaments (*arrows*) can be seen. *Bars* **a**, **c** 100 μm; **b**, **b'** 50 μm; **c** 25 μm; **d** 50 μm; **d inset** 13 μm; **e** 10 μm; **f** 100 μm; **g** 100 μm; **g'** 20 μm

were observed between the bundles of microfilaments (Fig. 5c).

Under in vitro and in vivo conditions, anti-Gal-1 disassembles Reissner fiber

The incubation of RF with anti-Gal-1 for 24 h reacted with the filaments forming RF and partially disassembled the fiber resulting in a reduction of its width (Fig. 7a, b).

Three hours after its injection into the CSF of adult rats, anti-Gal-1 was selectively detected in the pre-RF and in RF present in the Sylvius aqueduct and in the central canal of the spinal cord (Fig. 7c–i). In the injected rats, RF was fragmented and the pieces were twisted, forming tangles strongly reactive with anti-rabbit IgG. The tangles were seen close to the SCO and along the central canal of the spinal cord (Figs. 6b and 7e, f, g).

Galectin 1 is secreted by a discrete region of multiciliated ependyma of the third ventricle

In rats injected with anti-Gal-1 into the ventricular CSF, the antibody was tracked by using anti-rabbit IgG. The injected antibody was seen to react with a material located on the ventricular pole of multiciliated ependymal cells located in the most dorsal region of the lateral walls of the third ventricle (Fig. 7j–l). This region is adjacent to the SCO (Fig. 6b). Other regions of multiciliated ependyma were devoid of immunoreactive galectin 1 (Fig. 7k).

Discussion

The subcommissural organ (SCO) is an ancient and conserved brain gland characterized by specialized ependymal cells secreting into the ventricle glycoproteins that form the Reissner fiber (RF) (Nicholls 1913; Sterba 1969; Rodríguez et al. 1992, 1998). Despite the knowledge collected over a century, there are key questions on the SCO-RF complex not yet elucidated. The present findings contribute to further clarify the exceptional biosynthetic process of RF glycoproteins, to elucidate the RF proteome and *N*-glycome and to provide evidence to understand the polymerization processes of RF proteins. The substantial body of evidence harvested during a century (see Rodríguez and Oksche 1993) and some new information provided by the present paper have tempted us to outline the biography of SCO-spondin, the main protein forming RF.

Natural history of SCO-spondin, the main RF constituent: birth, storage, maturation, packaging, transport, release, gathering with partner molecules, working while traveling a long trip, aging and degradation

Birth SCO-spondin is a *N*-linked-sialoglycoprotein of 450 kDa (Nualart et al. 1991) with a multidomain organization (Gobron et al. 1996; Meiniel et al. 2008). It is synthetized as a precursor form of 540 kDa (Nualart et al. 1991). This precursor is a *N*-linked, high-mannose-type glycoprotein while stored in the RER (Diederen et al. 1987; Herrera and Rodríguez 1990; Meiniel and Meiniel 1985; Rodríguez et al. 1986). According to the present report, there are bi- and tri-antennary mannosyl cores that are the template for a large variety of *N*-linked complex-type carbohydrate chains (see below).

Proteins that enter the secretory pathway contain disulfide bonds within and between constituent polypeptide chains (Bulleid 2012; Feige and Hendershot 2011). Interestingly, thrombospondin (TSP)-1, a closely related molecule to SCO-spondin, is a homotrimer of disulfide-linked 150-kDa monomers (Hogg 2003). Early histochemical studies on the SCO indicated that the secretory material is rich in disulfide bonds. By using pseudoisocyanin, a fluorescent probe specific for disulfide bonds (Sterba 1962), G. Sterba and his group concluded that the proteins secreted by the SCO into the CSF are covalently linked by disulfide bonds (Sterba 1966, 1969; Sterba et al. 1967b; Wolf and Sterb 1972).

Storage Ever since the first ultrastructural study of the SCO (Afzelius and Olsson 1957), the landmark characteristic of the SCO cells of all species investigated, including human embryos, is the exceptional arrangement of the RER into numerous and large cisternae (Leatherland and Dodd 1968; Müller and Sterba 1965; Oksche 1969; Rodríguez et al. 1992, 1998; Stanka et al. 1964; Sterba 1966; Sterba et al. 1967a; Wenger et al. 1969; Ziegels 1976). The combined use of lectins and antibodies have shown that the bulk of material stored in RER

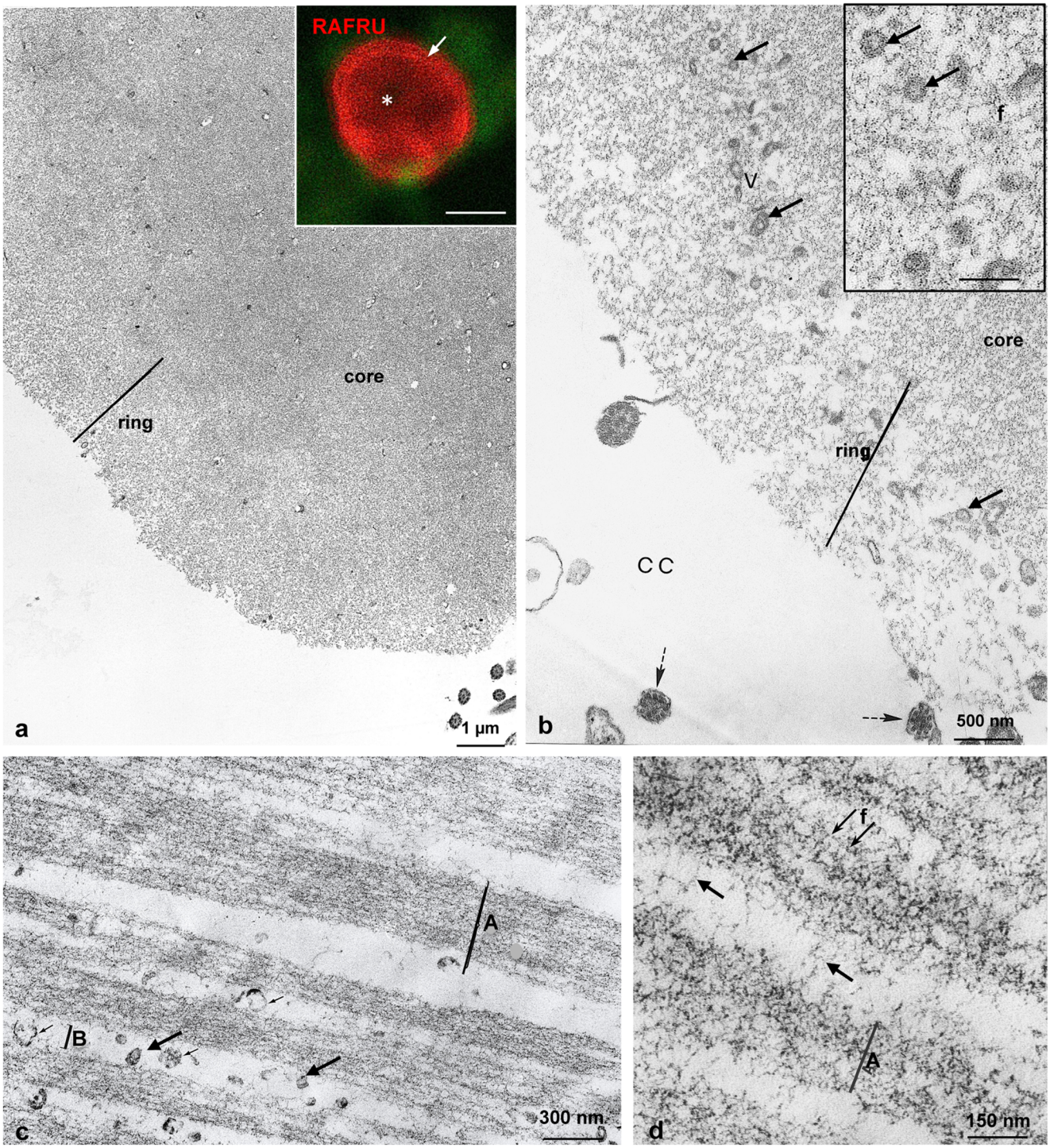

Fig. 5 Transmission electron microscopy of the bovine Reissner fiber. **a** Cross-section of Reissner fiber. RF displays different electron density in the core and the cortex. **Inset** The cortex (*arrow*) appears as a ring that is more strongly reactive with RAFRU than the core (*asterisk*). **b** Magnification of **a** showing that the core filaments are more densely packed than in the ring. Microvesicles (*arrows*) are concentrated at the border between the ring and core. *Broken arrows* cilia, *CC* central canal. **Inset** High magnification showing cross-sectioned filaments (*f*) and microvesicles displaying a three-layered membrane (unit of membrane, *arrows*). **c** Sagittal section of RF. Bundles (*A*) of microfilaments forming the RF are separated by electron lucent spaces (*B*) containing microvesicles (*arrows*). **d** High magnification of previous figure showing that microfilaments (*f, small arrows*) are packed into bundles (*A*) that are bridged by short filaments forming a honey comb-like structure (*large arrows*). *Bars*: **a** 1 μm; **a inset** 25 μm; **b** 500 nm; **c** 300 nm; **d** 150 nm

is the *N*-glycosylated SCO-spondin precursor form of 540 kDa (Herrera and Rodríguez 1990; Meiniel et al. 1988; Nualart and Rodríguez 1996; Nualart et al. 1991, 1998; Rodríguez et al. 1986, 1987a, b).

Previous investigations (Diederen and Vullings 1993; Diederen et al. 1987; Ermisch et al. 1968, 1971; Sterba et al. 1967b) and the present biosynthetic labelling study point to the existence of two pools of SCO-spondin molecules. Within a period of 20 min, a pool of SCO-spondin molecules is synthesized in the RER, transported to the Golgi apparatus, processed and packed into granules, behaving as a conventional secretory protein. The largest pool of SCO-spondin, however, remains in the lumen of large RER cisternae for long periods ranging from hours to days. Since these radiolabeled molecules will finally be processed through the Golgi apparatus, transported and released, they should be regarded as stored healthy precursor forms. The increasing radiolabelling of the RER compartments during the first 3 h after injection of ^{35}Cys into the CSF also indicates that the radioactive SCO-spondin continues to be synthetized *and* stored in the RER while the label is still present in the CSF (the CSF is renewed approximately every 4 h).

Maturation When moving from RER to the Golgi cisternae, the carbohydrate moiety and the protein backbone of SCO-spondin undergo processing; the latter is cleaved to a 450-kDa form while the high mannose-oligosaccharide is processed to a complex-type oligosaccharide (Nualart and Rodríguez 1996; Meiniel et al. 1988; Rodríguez et al. 1986, 1998). The present MS study of RF glycoproteins has shown a wealth of different complex-type oligosaccharides (see below).

Packaging The Golgi apparatus is a robust structure present along the axis of the supranuclear region of the SCO cells. Condensing vacuoles and immature secretory granules are surprisingly missing in the *trans*-Golgi region in all species investigated. Typical electron dense secretory granules are only seen in the ventricular cell pole (Rodríguez et al. 1998). A likely explanation is that, once formed, the secretory granules are quickly transported to the cell pole.

Transport The subapical (compartment 3) region of the SCO cells contains bundles of microtubules and few secretory granules. It may be regarded as the transport domain. Beyond this domain, the secretory granules accumulate at the ventricular cell pole as a small pool. Packaging of the secretory granules and their transport occur within a 20-min period after synthesis, as shown by the radiolabelling with ^{35}S-Cys and ^{3}H-Gal of compartments 2, 3 and 4. Since release of the radiolabeled secretion occurs between the first and the second hour after the ^{35}Cys/^{H3}Gal injection into the CSF, it may be suggested that upon their arrival to the apical cell pole, the secretory granules are stored here for up to 1 h.

Release into the CSF The SCO secretion is continuously discharged into the CSF where it starts an aggregation process (pre-RF) preceding the formation of RF. Pre-RF starts to be labeled sometime between the first and second hour after synthesis of the ^{35}Cys/^{H3}Gal labeled secretory proteins. Since ^{35}Cys/^{H3}Gal is available in the CSF for at least 4 h, it may be assumed that for a period of about 5–6 h postinjection, the labelling of pre-RF and RF proper is due to SCO-spondin that follows that rapid path. At variance, release of ^{35}Cys-labeled SCO-spondin several hours and days after ^{35}Cys administration could only correspond to radioactive SCO-spondin that after a long storage within RER enters the secretory pathway to be released. The fact that during the 5 days following the injection of ^{35}Cys, RF present in the Sylvius aqueduct and fourth ventricle is homogeneously radiolabeled indicates that during this period radioactive SCO-spondin stored in RER has *continuously* been released. The marked decrease of radioactivity in the RER 4d after the label injection and the labelling of the RF proximal end (see Fig. 2g) suggest that the RER stock of radioactive secretion is close to be depleted.

^{H3}Gal appears as a good marker of the rapidly releasable SCO-spondin. Since conjugation of galactose to the sugar chain occurs in the Golgi apparatus, pulse chasing of ^{H3}Gal appears as a good strategy to track the "rapid" SCO-spondin. Indeed, 1 and 3 h after its intraventricular administration, ^{H3}Gal labels the Golgi apparatus, the apical secretory granules and the *released* material forming pre-RF. Six hours after ^{H3}Gal injection, what in fact corresponds to 2 h after the label has been completely cleared from CSF, the Golgi apparatus is no longer labeled but the apical secretory granules and pre-RF are. After 1d of being injected, ^{H3}Gal was completely missing from the SCO cells while ^{35}Cys strongly labeled all compartments of the secretory pathway, indicating that when the ^{35}Cys-labeled SCO-spondin molecules that had been stored in the RER for 1d entered the Golgi cisternae, ^{H3}Gal was longer available. It may be suggested that the ^{35}Cys+, ^{H3}Gal + secretion corresponds to the "rapid" SCO-spondin and the ^{35}Cys+, ^{H3}Gal- secretion corresponds to SCO-spondin stored in the RER that becomes slowly and progressively releasable.

What is the mechanism leading to a small pool of SCO-spondin to rapidly enter the secretory pathways while most of the SCO-spondin molecules are stored for hours or days before entering the secretory pathway? What are the signals, either extracellular or intracellular, driving this complex clock? The functional significance of this unique property of SCO cells remains a challenge.

Association The SCO-spondin molecules released into the CSF undergo a progressive process of aggregation, first as flocculated material on top of the cilia (Schöbitz et al. 2001; Wenger et al. 1969), then forming loose fibrils, the "origin fibers" (*Ursprungsfäden*, Nicholls 2013; Sterba et al. 1967a), later a mesh of fibrils on the whole surface of the SCO ("pre-RF," Rodríguez et

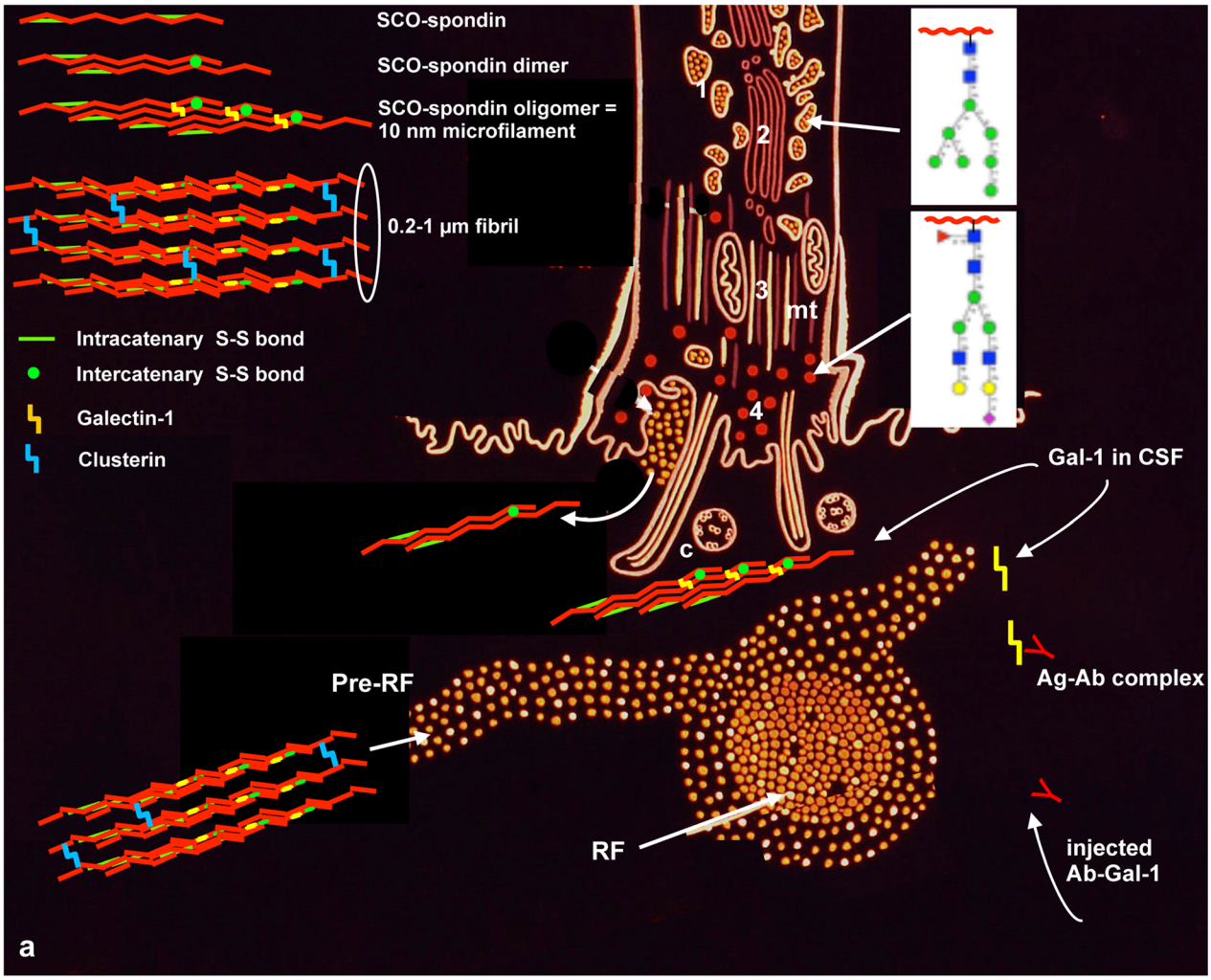
SCO-spondin
SCO-spondin dimer
SCO-spondin oligomer = 10 nm microfilament
0.2-1 μm fibril
Intracatenary S-S bond
Intercatenary S-S bond
Galectin-1
Clusterin
1
2
3
mt
4
c
Gal-1 in CSF
Ag-Ab complex
Pre-RF
RF
injected Ab-Gal-1
a

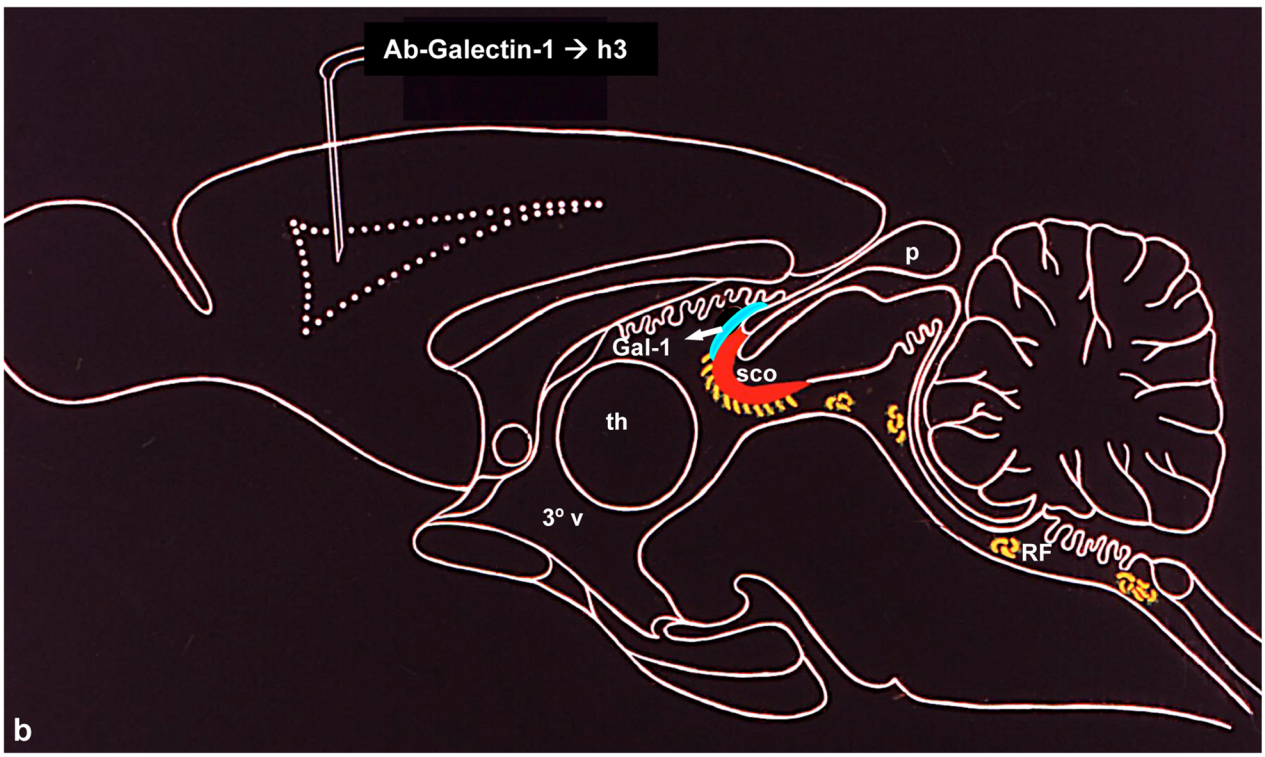
Ab-Galectin-1 → h3
p
Gal-1
sco
th
3° v
RF
b

◀ **Fig. 6** Summary of findings. In the rough endoplasmic reticulum SCO-spondin is synthetized and *N*-glycosylated with oligosaccharides rich in mannose and glucose (*1*) and further glycosylated in the Golgi apparatus (*2*) to form secretory granules that are transported by microtubules (*3*, *mt*) to the cell pole (*4*). SCO-spondin is released as dimers formed by intercatenary disulfide bonds (*green dot*). On top of the cilia (*c*), SCO-spondin dimers are cross-linked into oligomers by Gal-1 (*yellow hook*) present in the CSF. This oligomers correspond to the 10-nm microfilaments visualized with transmission electron microscopy. These microfilaments are further packed into fibrils by the action of clusterin (*blue hook*). In turn, fibrils are densely packed to form the Reissner fiber proper (*RF*). Gal-1 (*yellow hook*), secreted into the CSF by ependymal cells close to the SCO, is present in RF. Antibodies anti-Gal-1 injected into the CSF interferes the assembly of pre-RF fibrils and of RF. **b** In the adult rat, a single injection into the CSF of antibodies against Gal-1 blocks the addition of the newly released SCO-spondin molecules resulting in the detachment of RF from the SCO and its fragmentation (*yellow*). Ependymal cells located close to the SCO (*green*) secrete Gal-1 into the third ventricle. *3°v* third ventricle, *p* pineal, *th* thalamus

al. 1986, 1987a) and finally into RF proper (Sterba et al. 1967a). The present pulse-chase labelling study has shown that the aggregation process from pre-RF to RF takes about 1–2 h.

What is the mechanism underlying the progressive packaging of the proteins secreted by the SCO? There is strong evidence that RF glycoproteins, once released, form intercatenary disulfide bonds leading to the formation of pre-RF (Wolf and Sterb 1972). The role of disulfide bonds in the assembly of RF is strongly supported by the disaggregation and re-aggregation of isolated bovine RF using oxidative and reducing agents (Wolf and Sterb 1972). Disulfide bonds can be cleaved in the extracellular environment and this cleavage may be reversible, a mechanism frequently used for controlling protein function (Hogg 2003). Disulfide cleavage was first described in thrombospondin-1 (Hogg 2003), a protein closely related to SCO-spondin. If this mechanism operates in SCO-spondin, it would explain the presence in the CSF of soluble proteins reacting with anti-SCO-spondin (Vío et al. 2008).

A series of experiments has demonstrated that the aggregation of RF proteins into fibrils and pre-RF depends on SCO-intrinsic factors other than disulfide bonding and that the full packaging of proteins forming the RF proper depends on partner molecules extrinsic to the SCO but present in the CSF (Hoyo-Becerra et al. 2005; Rodríguez et al. 1989, 1999a; Schöbitz et al. 1986, 2001). What is the nature of these putative intrinsic and extrinsic factors?

Gathering with partner molecules Is there an intrinsic partner molecule involved in the aggregation process? *Clusterin* is a good candidate. According to the present investigation, clusterin is a constituent protein of RF. Clusterin is a *N*-glycosylated protein with five disulfide bridges, with an apparent mass of 70–80 kDa. Under normal conditions, clusterin is constitutively secreted from cells and is found in extracellular fluids (Wilson and Zoubeidi 2016). Immunohistochemical studies have revealed the occurrence of clusterin as a granule component of neuroendocrine cells (Jenne and Tschopp 1992). Although present in RF, the presence of clusterin in the SCO cells has yet to be investigated.

Galectin 1 (Gal-1): What is the nature of the CSF molecule(s), extrinsic to the SCO, involved in the highest degree of aggregation of RF proteins? The present MS analysis revealed Gal-1 to be present in the freshly collected bovine RF. Furthermore, in vitro incubation of the bovine RF with antibodies against Gal-1 resulted in its partial disassembly and the same antibody injected into the CSF of rats specifically bound to RF and resulted in its fragmentation.

Gal-1 is a non-covalent homodimeric protein, with a 14-kDa monomer containing one carbohydrate-recognizing domain (Elola et al. 2005). It occurs as a non-covalent homodimer widely expressed in many tissues. Gal-1 is present extracellularly and intracellularly. It is an atypical secreted protein (Elola et al. 2005) that does not pass along the standard endoplasmic reticulum/Golgi pathway.

The following evidence supports that Gal-1 does participate in the packaging of RF by cross-linking SCO-spondin molecules as they are released into the CSF. (i) Gal-1 exists as a dimer in solution (Camby et al. 2006; Leppänen et al. 2005); it is present in plasma (He et al. 2017). Dimerized Gal-1 has the property to crosslink glycoproteins (Earl et al. 2011). Gal-7 and Gal-9 have been detected in the human CSF (Burman and Svenningsson 2016; Dumont et al. 2004). (ii) After being secreted, Gal-1 has several partner proteins, thrombospondin is one of them (Moiseeva et al. 2000). (iii) Gal-1 binds α2–3 sialylated glycans (Patnaik et al. 2005; Stowell et al. 2006). Since the majority of sialic acids identified in RF proteins are α(2–3) linked (present report), it seems likely that Gal-1 binds to the glycans of SCO-spondin. (iv) RF formation is blocked by intraventricular administration of anti-Gal-1, closely resembling the blockage of RF formation by a single injection into the CSF of an antiserum against RF proteins (S. Rodríguez et al. 1990).

What is the source of Gal-1 found in RF? In Gal-1 secreting neurons, Gal-1 is confined to the surface and/or extracellular region (Sango et al. 2004), reflexing the atypical mechanism of secretion via inside-out transportation translocation across the plasma membrane (Camby et al. 2006). Anti-Gal-1 injected into the CSF immunoreacts with a material located in the apical plasma membrane domain of a small population of multiciliated ependymal cells of the third ventricle. The possibility that a small source of Gal-1 is located close and rostral to the SCO and that the CSF entering the Sylvius aqueduct quickly conveys Gal-1 to the site of release of SCO-spondin seems fascinating. Interestingly, expression of Gal-1 has been reported in neurons of the pineal gland and in the

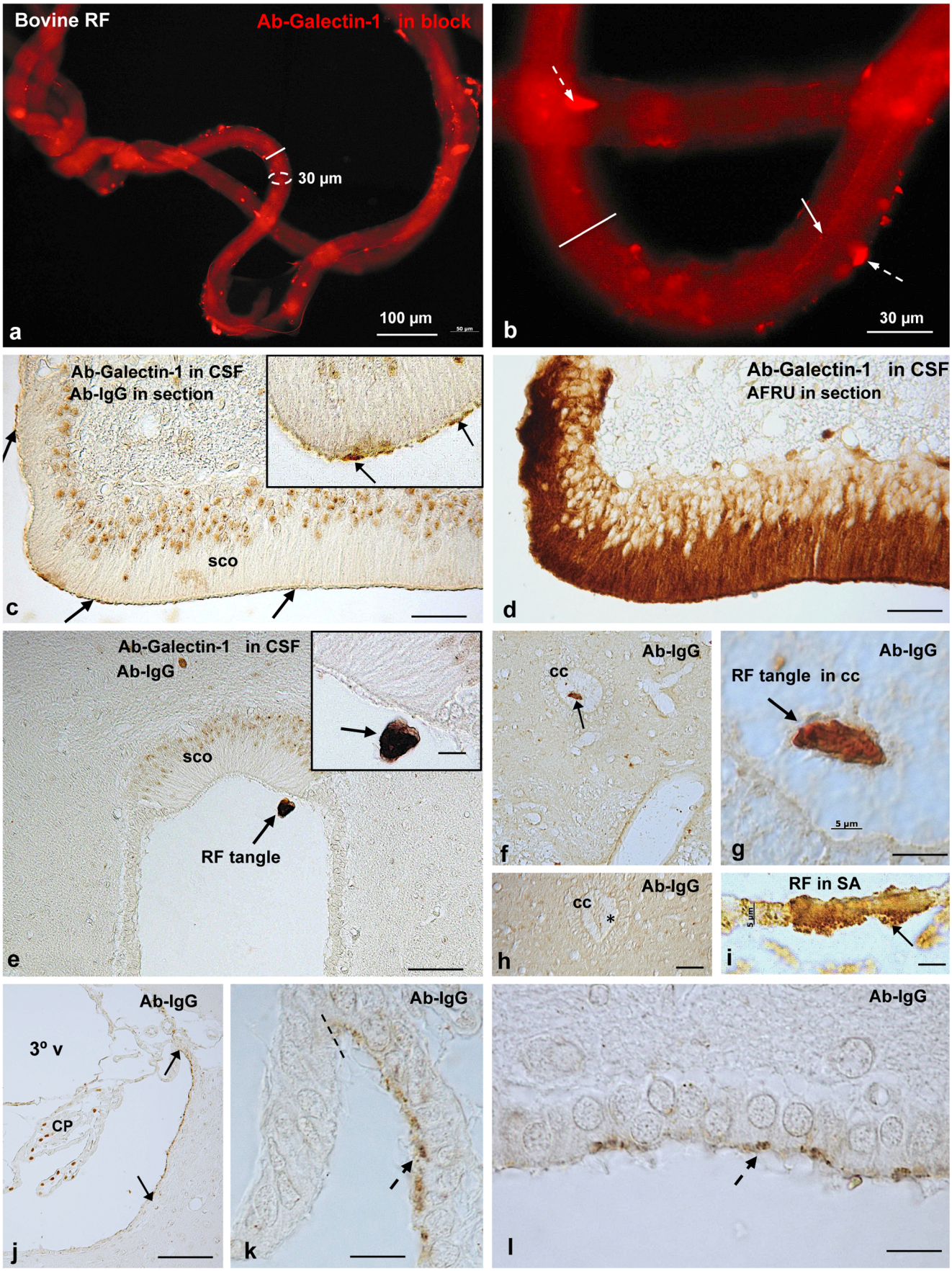
Bovine RF
Ab-Galectin-1 in block
30 μm
100 μm
a
b
30 μm
Ab-Galectin-1 in CSF
Ab-IgG in section
sco
c
Ab-Galectin-1 in CSF
AFRU in section
d
Ab-Galectin-1 in CSF
Ab-IgG
sco
RF tangle
e
Ab-IgG
cc
f
Ab-IgG
RF tangle in cc
5 μm
g
Ab-IgG
cc
*
h
RF in SA
5 μm
i
Ab-IgG
3° v
CP
j
Ab-IgG
k
Ab-IgG
l

◀ **Fig. 7** Antibodies against galectin-1 disassemble Reissner fiber. **a**, **b** In block immunostaining with anti-galectin-1. The antibody reacts with filaments (*full arrow*) and patches of material on the surface of RF (**b**, *broken arrow*). The incubation of RF with anti-galectin-1 for 24 h partially disassembles RF resulting in a reduction of its width from 50 to 30 μm, (**a**). **c**, **l** Injection of anti-galectin-1 into the CSF of adult rats and detection of the injected antibody by using anti-rabbit IgG in the sections. **c**, **d** Adjacent sagittal sections of the SCO of a rat injected with anti-galectin-1, incubated with anti-IgG (incomplete immunostaining, **c**) or with AFRU (**d**). Ag-Ab complex are shown on the surface of SCO cells (*arrows*). This is best shown in **inset** (*arrows*). **e** Frontal section of the SCO of a rat injected in vivo with anti-galectin-1, incubated with anti-IgG. RF is free into the ventricular lumen, rolled as a tangle (*arrow*). **Inset** High magnification of tangled RF showing the selective binding of the injected antibody (*arrow*). **f**, **g**, **h** Frontal sections of the spinal cord of a rat injected in vivo with anti-galectin 1, incubated with anti-IgG. There are levels of the spinal cord where RF is missing (**h**) while in others RF appears as rolled tangles (**f**, **g**). **i** In sagittal sections of the Sylvius aqueduct, fragments of RF with patches of material that had reacted with the injected antibody are seen (*arrow*). **j**, **l** Frontal section through the dorsal region of the third ventricle (*3°v*) of a rat injected in vivo with anti-galectin-1. Incomplete immunostaining using anti-IgG in the section. In a discrete region of the third ventricle delimited by the *arrows* in **j**, the multiciliated ependymal cells have immunoreactive material on their ventricular pole (*broken arrow* in **k**, **l**). *CP* choroid plexus. **k** Close to the dorsal wall of the ventricle there is a sharp limit between immunoreactive and non-immunoreactive ependyma (*broken arrow*). **l** More ventral, immunoreactive and non-immunoreactive ependymal cells are intermingled. *Bars*: **a** 100 μm; **b** 30 μm; **c**, **d** 20 μm; **e**, **f**, **h** 40 μm; **g** 10 μm; **i** 5 μm; **j** 100 μm; **k**, **i** 10 μm

choroid plexus (Akazawa et al. 2004; Sango et al. 2004), two circumventricular organs.

Briefly, RF may be regarded as the result of a dynamic process involving interactions between SCO-spondin and Gal-1 at different levels of organization. Gal-1 could provide the scaffolding for oligomeric assemblies of SCO-spondin; SCO-spondin may assemble into higher-order clusters through intercatenary disulfide bonds, direct Gal-1-protein interactions and the clustering effect of clusterin (Fig. 6). Amazingly, half a century ago, Sterba proposed that RF is formed by a high molecular weight secretion from the SCO and a low molecular weight substance from the CSF (Sterba 1969; Wolf and Sterb 1972).

Other members of RF: the proteomic analysis also showed the presence in RF of calmodulin, S100β, creatine kinase B-type, α-tubulin and β-tubulin. While S100β is co-expressed by a subpopulation of the SCO-spondin secreting cells of the SCO (present report), there is no evidence on the source of calmodulin present in RF. The pattern of immunostaining of S100β as patches located at the periphery of RF indicates that S100β is associated to RF but it does not participate in RF polymerization. Since calmodulin and S100β are members of a family of Ca2 + −binding proteins (Haeseleer and Palczewski 2002; Heizmann and Cox 1998), they might regulate the concentration of calcium in the microenvironment of RF, the long and slender central canal of the spinal cord in particular. B-type creatine kinase is the cytosolic brain-type isoform of a well established energy buffering and shuttling system. There is evidence that creatine kinase isoforms associate with proteins at sites of ATP delivery and consumption (Schlattner et al. 2016). Whereas B-type creatine kinase has often been found concentrated at the inner site of the plasma membrane where it is coupled with ATP-consuming reactions, its extracellular location has not yet been described. Moreover, there is no evidence that RF formation is ATP dependent. Transmission electron microscopy provided evidence for microvesicles migrating between the fibrils of RF (Fig. 5). These microvesicles could be the source of the identified B-type creatine kinase as well as tubulin isoforms. Both proteins represent abundant cytosolic proteins of neurons and glial cells and might be constituents of exosomes derived from these cells.

How does the protein composition matche with the macromolecular organizations of RF? Along the vertebrate phylum, the elemental components of RF are wavy microfilaments about 10 nm thick, running longitudinally (Afzelius and Olsson 1957; Hoheisel et al. 1971; Kohno 1969; Müller and Sterba 1965; Rodríguez 1970; Rodríguez and Caprile 2001; Sterba and Naumann 1966). Since the same microfilaments are also the elemental component of pre-RF, they most likely correspond to oligomers of SCO-spondin. Although speculative, it may be proposed that SCO-spondin is first oligomerized into microfilaments by the action of sulphide bridging and the cross-linking action of Gal-1; these microfilaments would be further packed into 0.2- to 1-μm-thick filaments (Sterba et al. 1967c) by the horizontally oriented 7-nm microfilaments (clusterin?) (Fig. 6a).

Working while traveling a long trip RF grows rostro-caudally by the permanent aggregation of newly released SCO-spondin molecules (Sterba 1969; Rodríguez et al. 1987b, 1992; Sterba et al. 1967a). After a few hours of administration, ^{35}S-cys-labeled material appears in RF (Ermisch 1973; Diederen and Vullings 1993; Ermisch et al. 1968; Sterba et al. 1967b, present report). With increasing time after injection, more distal segments of RF become progressively labeled, until the entire length of RF is labeled. This has allowed to determine the growth rate of RF in various species. In the mouse, RF grows 10% of its total length per day (Ermisch 1973). Thus, the life span of a SCO-spondin molecule, since its synthesis to the arrival to its final destination in the terminal ventricle, is around 15 days.

What do the RF molecules do while traveling along the cerebral aqueduct, fourth ventricle and the whole length of the spinal cord? RF participates in the regulation of the CSF concentration of monoamines either by binding and transporting them away (l-DOPA, noradrenaline, adrenaline), or by transiently binding them and releasing them back to the CSF (serotonin) (Hess and Sterba 1973; Caprile et al. 2003;

Ermisch et al. 1970). Adrenaline and noradrenaline share the same binding site corresponding to a repeated sequence present in SCO-spondin, while serotonin has its own binding site (Caprile et al. 2003). RF-deprived rats by immunoneutralization with anti-SCO-spondin have an increased CSF concentration of bioamines (S Rodríguez et al. 1999b).

The complex multidomain structure of SCO-spondin, the surprising variety and complexity of *N*-glycan structures (present report) and its amazing journey through the CSF suggest that this molecule, in the manner of a cargo train with numerous wagons, is engaged in the CSF concentration and clearance of numerous compounds (in addition to biogenic amines), yet to be investigated.

Aging and degradation At the distal end of the spinal cord, the central canal becomes dilated, forming the terminal ventricle (Olsson 1955). At this site, RF ends as a jelly mass known as massa caudalis (Olsson 1955; Oksche 1969). When passing from the RF stage to the massa caudalis stage, RF glycoproteins become unpacked and undergo chemical modifications associated to a rich local battery of enzymes (Naumann 1968). A key modification is the loss of sialic acid residues, exposing galactose as terminal residue (Rodríguez et al. 1987a, b, c). The modified RF glycoproteins escape from the terminal ventricle by openings in the dorsal wall and appear to reach lymphatic vessels (Peruzzo et al. 1987). However, the important question of the final fate of RF glycoproteins and their cargo (the compound bound to SCO-spondin), beyond the terminal ventricle, is an open question.

Evolutionary history of SCO-spondin, a protein 770 million years old

The SCO is present throughout the evolution of chordates, from amphioxus (Olsson 1955; Olsson and Wingstrand 1954; Rodríguez and Oksche 1993) to man (Oksche 1969; Rodríguez et al. 2001). The tunicate *Oikopleura dioica*, which merges at the bottom of the ocean over 770 million years ago, already has a single cell secreting a very thin Reissner fiber (Olsson 1958, 1972, 1993) that immunoreacts with antibodies against mammalian RF glycoproteins (Olsson et al. 1994). RF represents a very conserved design, with the same fundamental pattern in all members of the vertebrate phylum and a remarkable conservation of the nature of the proteins contributing to its formation (Gobron et al. 1999; Helm et al. 2017; Olsson 1993; Rodríguez et al. 1992). The SCO-spondin gene is traceable from deuterostomes to humans, as a single copy that could be modified as a result of exon shuffling in ancestral chordates (Creveaux et al. 1998; Helm et al. 2017; Kawashima et al. 2009). Thus, the ancient SCO-spondin may be considered a member of an exclusive group of proteins accompanying the brain through its long lasting evolution.

The large molecular size of SCO-spondin, its conserved sequence along evolution, its multidomain structure and the complexity and variety of *N*-glycan structures demonstrated in the present research characterize SCO-spondin as an ancestral secretion exhibiting molecular plasticity and multiplicity of functions in an emerging brain that will evolve toward a more complex, hierarchy and sophisticated central nervous system.

Acknowledgements The authors wish to acknowledge FRIVAL Ltda. (Valdivia) and the valuable technical support of Mr. Genaro Alvial and Yvonne Ducho and the Confocal and Electron Microscopy Core Facilities of Universidad Austral de Chile. The study was supported by Fondecyt 1000435, 1070241 and 1111018 to EMR.

Abbreviations AFRU, Antisera raised in rabbits against isolated bovine fiber of Reissner dissolved in urea; CSF, Cerebrospinal fluid; Gal-1, Galectin-1; RER, Rough endoplasmic reticulum; RF, Reissner fiber; SA, Aqueduct of Sylvius; SCO, Subcommissural organ

References

Afzelius BA, Olsson R (1957) The fine structure of the subcommissural organ cells and Reissner's fibre in Myxine. Z Zellforsch Mikrosk Anat 46:672–685

Akazawa C, Nakamura Y, Sango K, Horie H, Kohsaka S (2004) Distribution of the galectin-1 mRNA in the rat nervous system: its transient upregulation in rat facial motor neurons after facial nerve axotomy. Neuroscience 125:171–178

Attila U, Talanti S (1973) Incorporation of 35 S-labelled cysteine in the subcommissural organ of the rat after adrenalectomy and after treatment with hydrocortisone. Acta Physiol Scand 87:422–424

Bulleid NJ (2012) Disulfide bond formation in the mammalian endoplasmic reticulum. Cold Spring Harb Perspect Biol 4:a013219

Burman J, Svenningsson A (2016) Cerebrospinal fluid concentration of Galectin-9 is increased in secondary progressive multiple sclerosis. J Neuroimmunol 292:40–44

Camby I, Le Mercier M, Lefranc F, Kiss R (2006) Galectin-1: a small protein with major functions. Glycobiology 16:137R–157R

Caprile T, Hein S, Rodríguez S, Montecinos H, Rodríguez EM (2003) Reissner fiber binds and transports away monoamines present in the cerebrospinal fluid. Brain Res Mol Brain Res 110:177–192

Ceroni A, Maass K, Geyer H, Geyer R, Dell A, Haslam SM (2008) GlycoWorkbench: a tool for the computer-assisted annotation of mass spectra of glycans. J Proteome Res 7:1650–1659. https://doi.org/10.1021/pr7008252

Cifuentes M, Rodríguez S, Pérez J, Grondona JM, Rodríguez EM, Fernández-Llebrez P (1994) Decreased cerebrospinal fluid flow through the central canal of the spinal cord of rats immunologically deprived of Reissner's fibre. Exp Brain Res 98:431–440

Creveaux I, Gobron S, Meiniel R, Dastugue B, Meiniel A (1998) Complex expression pattern of the SCO-spondin gene in the bovine subcommissural organ: toward an explanation for Reissner's fiber complexity? Brain Res Mol Brain Res 55:45–53

Diederen JHB, Vullings HGB (1993) Dynamic aspects of the secretory process in the amphibian subcommissural organ. In: Oksche A, Rodríguez EM, Fernández-Llebrez P (eds) The subcommissural organ. Springer, Berlin, pp 111–119

Diederen JHB, Vullings HGB, Legerstee-Oostveen GG (1987) Autoradiographic study of the production of secretory material by the subcommissural organ of frogs (*Rana temporaria*) after injection

of several radioactive precursors, with special reference to the glycosilation and turnover rate of the secretory material. Cell Tissue Res 248:215–222

Dumont D, Noben JP, Raus J, Stinissen P, Robben J (2004) Proteomic analysis of cerebrospinal fluid from multiple sclerosis patients. Proteomics 4:2117–2124

Earl LA, Bi S, Baum LG (2011) Galectin multimerization and lattice formation are regulated by linker region structure. Glycobiology 21:6–12

Elola MT, Chiesa ME, Fernández Alberti A, Mordoh J, Fink NE (2005) Galectin-1 receptors in different cell types. J Biomed Sci 12:13–29. https://doi.org/10.1007/s11373-004-8169-5

Ermisch A (1973) Zur Charakterisierung des Komplexes Subcommisuralorgan-Reissnerschen Faden und seiner Beziehung zum Liquor unter besonderer Berücksichtigung autoradiographischer Untersuchungen sowie funktioneller Aspekte. Wiss Z Karl-Marx-Univ Leipzig Mat Naturwiss R 22: 297–336

Ermisch A, Sterba G, Hartmann G, Freyer K (1968) Autoradiographische Untersuchungen über das Wachstum des Reissnerschen Fadens von Cyprinus carpio (L.). Z Zellforsch Mikrosk Anat 91:220–235

Ermisch A, Sterba G, Hess J (1970) Untersuchungen zur Klärung der Funktion des Reissnerschen Fadens. In-vitro-Bindung von Noradrenalin, Adrenalin und Serotonin. Experientia 26:1319–1321

Ermisch A, Sterba G, Mueller A, Hess J (1971) Autoradiographische Untersuchungen am Subcommissuralorgan und dem Reissnerschen Faden. I. Organsekretion und Parameter der Organleistung als Grundlagen zur Beurteilung der Organfunktion. Acta Zool 52:1–21

Feige MJ, Hendershot LM (2011) Disulfide bonds in ER protein folding and homeostasis. Curr Opin Cell Biol 23:167–175. https://doi.org/10.1016/j.ceb.2010.10.012

Gobron S, Monnerie H, Meiniel R, Creveaux I, Lehmann W, Lamalle D, Dastugue B, Meiniel A (1996) SCO-spondin: a new member of the thrombospondin family secreted by the subcommissural organ is a candidate in the modulation of neuronal aggregation. J Cell Sci 109: 1053–1061

Gobron S, Creveaux I, Meiniel R, Didier R, Dastugue B, Meiniel A (1999) Sco-spondin is evolutionarily conserved in the central nervous system of the chordate phylum. Neuroscience 88:655–664

Gobron S, Creveaux I, Meiniel R, Didier R, Herbet A, Bambdad M, El Bitar F, Dastugue B, Meiniel A (2000) Subcommissural organ/Reissner's fibre complex: characterization of SCO-spondin a glycoprotein with potent activity on neurite outgrowth. Glia 32:177–191

Haeseleer F, Palczewski K (2002) Calmodulin and Ca2+-binding proteins (CaBPs): variations on a theme. Adv Exp Med Biol 514:303–317

He XW, Li WL Li C, Liu P, Shen YG, Zhu M, Jin XP (2017) Serum levels of galectin-1, galectin-3, and galectin-9 are associated with large artery atherosclerotic stroke. Sci Rep. https://doi.org/10.1038/srep40994

Heizmann CW, Cox JA (1998) New perspectives on S100 proteins: a multi-functional Ca(2+)-, Zn(2+)- and Cu(2+)-binding protein family. Biometals 11:383–397

Helm C, Karl A, Beckers P, Kaul-Strehlow S, Ulbricht E, Kourtesis I, Kuhrt H, Hausen H, Bartolomaeus T, Reichenbach A, Bleidorn C (2017) Early evolution of radial glial cells in Bilateria. Proc R Soc B 284(20170743). https://doi.org/10.1098/rspb.2017.0743

Hennig R, Cajic S, Borowiak M, Hoffmann M, Kottler R, Reichl U, Rapp E (2016) Towards personalized diagnostics via longitudinal study of the human plasma N-glycome. Biochim Biophys Acta 1860:1728–1738

Herrera H, Rodríguez EM (1990) Secretory glycoproteins of the rat subcommissural organ are N-linked complex-type glycoproteins. Demonstration by combined use of lectins and specific glycosidases, and by administration of Tunicamycin. Histochem 93:607–615

Hess J, Sterba G (1973) Studies concerning the function of the complex subcommissural organ-liquor fibre: the binding ability of the liquor fibre to pyrocatechin derivatives and its functional aspects. Brain Res 58:303–312

Hogg PJ (2003) Disulfide bonds as switches for protein function. Trends Biochem Sci. https://doi.org/10.1016/S0968-0004(03)00057-4

Hoheisel G, Sterba G, Ermisch A (1971) Feinstruktur des isolierten Reissnerschen Fadens vom Rind. J Hirnforsch 13:33–38

Hoyo-Becerra C, López-Avalos MD, Alcaide-Gavilán M, Gómez-Roldán MC, Pérez J, FernándezLlebrez P, Grondona JM (2005) Reissner's fiber formation depends on developmentally regulated factors extrinsic to the subcommissural organ. Cell Tissue Res 321:429–441

Irigoin C, Rodríguez EM, Heinrichs M, Frese K, Herzog S, Oksche A, Rott R (1990) Immunocytochemical study of the subcommissural organ of rats with induced postnatal hydrocephalus. Exp Brain Res 82:384–392

Jenne DD, Tschopp J (1992) Clusterin: the intriguing guises of a widely expressed glycoprotein. Trends Biochem Sci 17:154–159

Kähne T, Richter S, Kolodziej A, Smalla KH, Pielot R, Engler A, Ohl FW, Dieterich DC, Seidenbecher C, Tischmeyer W, Naumann M, Gundelfinger ED (2006) Proteome rearrangements after auditory learning: high-resolution profiling of synapse-enriched protein fractions from mouse brain. J Neurochem 138:124–138

Kawashima T, Kawashima S, Tanaka C, Murai M, Yoneda M, Putnam NH, Rokhsar DS, Kanehisa M, Satoh N, Wada H (2009) Domain shuffling and the evolution of vertebrates. Genome Res 19:1393–1403

Kohno K (1969) Electron microscopic studies on Reissner's fiber and the ependymal cells in the spinal cord of the rat. Z Zellforsch Mikrosk Anat 94:565–573

Leatherland JF, Dodd JM (1968) Studies on the structure,ultrastructure and function of the subcommissural organ-Reissner's fibre complex of the European eel Anguilla anguilla L. Z Zellforsch Mikros Anat 89:533–549

Leppänen A, Stowell S, Blixt O, Cummings RD (2005) Dimeric galectin-1 binds with high affinity to α2,3-sialylated and non-sialylated terminal *n*-acetyllactosamine units on surface-bound extended glycans. J Biol Chem 280:5549–5562. https://doi.org/10.1074/jbc.M412019200

Meiniel R, Meiniel A (1985) Analysis of the secretions of the subcommissural organs of several vertebrate species by use of fluorescent lectins. Cell Tissue Res 239:359–364

Meiniel A, Molet JL, Meiniel R (1988) Complex-type glycoproteins synthesized in the subcommissural organ of mammals. Light- and electron-microscopic investigations by use of lectins. Cell Tissue Res 253:383–395

Meiniel R, Molat JL, Duchier-Liris N, Meiniel A (1990) Ontogenesis of the secretory epithelium of the bovine subcommissural organ. A histofluorescence study using lectins and monoclonal antibodies. Brain Res Dev Brain Res 55:171–180

Meiniel O, Meiniel R, Lalloué F, Didier R, Jauberteau MO, Meiniel A, Petit D (2008) The lengthening of a giant protein: when, how, and why? J Mol Evol 66:1–10

Moiseeva EP, Javed Q, Spring EL, de Bono DP (2000) Galectin 1 is involved in vascular smooth muscle cell proliferation. Cardiovasc Res 45:493–502

Müller H, Sterba G (1965) Elektronenmikroskopische Untersuchungen des Subkommissuralorganes von Lampreta planeri (Bloch). Verh Dtsch Zool Ges Jena,Zool Anz Suppl 23:441–453

Naumann W (1968) Histochemische Untersuchungen am Subkommissuralorgan und Reissnerschen Faden von Lampreta planeri (Bloch). Z Zellforsch Mikrosk Anat 87:572–591

Nicholls GE (1913) The structure and development of Reissner's fibre and sub-commissural organ. Part 1. Q J Microsc Sci 58(part 1):1–116

Nualart F, Hein S (2001) Biosynthesis and molecular biology of the secretory proteins of the subcommissural organ. Microsc Res Tech 52:468–483

Nualart F, Rodríguez EM (1996) Immunochemical analysis of the subcommissural organ-Reissner's fiber complex using antibodies against alkylated and deglycosylated bovine Reissner's fiber glycoproteins. Cell Tissue Res 286:23–31

Nualart F, Hein S, Rodríguez EM, Oksche A (1991) Identification and partial characterization of the secretory glycoproteins of the bovine subcommissural organ-Reissner's fiber complex. Evidence for the existence of two precursor forms. Brain Res Mol Brain Res 11: 227–238

Nualart F, Hein S, Yulis CR, Zárraga AM, Araya A, Rodríguez EM (1998) Partial sequencing of Reissner's fiber glycoprotein I (RF-Gly I). Cell Tissue Res 292:239–250

Oksche A (1961) Vergleichende Untersuchungen über die sekretorische Aktivität des Subkommissuralorgans und den Gliacharakter seiner Zellen. Z Zellforsch Mikrosk Anat 54:549–612

Oksche A (1969) The Subcommissural Organ. J Neuro Visc Rel Suppl. IX:111–139

Oksche A, Rodríguez EM, Fernández-Llebrez P (1993) The subcommissural organ. Springer, Berlin, pp 41–49

Olsson R (1955) Structure and development of Reissner's fibre in the caudal end of amphioxus and some lower vertebrates. Acta Zool (Stockh) 36:167–198

Olsson R (1958) Studies on the subcommissural organ. Acta Zool (Stockh) 39:71–102

Olsson R (1972) Reissner's fiber in ascidian tadpole larvae. Acta Zool (Stockh) 53:17–21

Olsson R (1993) Reissner's fiber mechanisms: some common denominators. In: Oksche A, Rodríguez EM, Fernández-Llebrez P (eds) The subcommissural organ. Springer, Berlin, pp 33–39

Olsson R, Wingstrand KG (1954) Reissner's fibre and the infundibular organ in amphioxus. Results obtained with Gomori's chrome alum haematoxylin. Univ Bergen Arbok (Publ Biol Stat) 14:1–14

Olsson R, Yulis CR, Rodríguez EM (1994) The infundibular organ of the lancelet (*Branchiostoma lanceolatum*, Acrania): an immunocytochemical study. Cell Tissue Res 277:107–114

Ortloff AR, Vío K, Guerra M, Jaramillo K, Kaehne T, Jones H, McAllister JP, Rodríguez EM (2013) Role of the subcommissural organ in the pathogenesis of congenital hydrocephalus in the HTx rat. Cell Tissue Res 352:707–725

Patnaik SK, Potvin B, Carlsson S, Sturm D, Leffler H, Stanley P (2005) Complex *N*-glycans are the major ligands for galectin-1, -3, and -8 on Chinese hamster ovary cells. Glycobiology 16:305–317

Peruzzo B, Rodríguez S, Delannoy L, Hein S, Rodríguez EM (1987) Ultrastructural immunocytochemical study of the massa caudalis of lamprey larvae (*Geotria australis*). Evidence for the vascular fate of Reissner's fiber material. Cell Tissue Res 247:367–376

Rodríguez EM (1969) Fixation of the central nervous system by perfusion of the cerebral ventricles with a threefold aldehyde mixture. Brain Res 15:395–412

Rodríguez EM (1970) Ependymal specializations. II. Ultrastructural aspects of the apical secretion of the toad subcommissural organ. Z Zellforsch Mikrosk Anat 111:15–31

Rodríguez S, Caprile T (2001) Functional aspects of the subcommissural organ-Reissner's fiber complex with emphasis in the clearance of brain monoamines. Microsc Res Tech 52:564–572

Rodríguez EM, Oksche A (1993) Historical landmarks in the investigations of the subcommissural organ and Reissner's fiber. In: Oksche A, Rodríguez EM, Fernández-Llebrez P (eds) The subcommissural organ. Springer, Berlin, pp 9–19

Rodríguez EM, Oksche A, Hein S, Rodríguez S, Yulis R (1984a) Comparative immunocytochemical study of the subcommissural organ. Cell Tissue Res 237:427–441

Rodriguez EM, Yulis CR, Peruzzo B, Alvial G, Andrade R (1984b) Standardization and silver methenamine for light and electron microscopy immunocytochemistry. Histochemistry 81:253–263

Rodríguez EM, Herrera H, Peruzzo B, Rodríguez S, Hein S, Oksche A (1986) Light- and electron microscopic immunocytochemistry and lectin histochemistry of the subcommissural organ: evidence for processing of the secretory material. Cell Tissue Res 243:545–559

Rodríguez EM, Oksche A, Rodríguez S, Hein S, Peruzzo B, Schoebitz K, Herrera H (1987a) The subcommissural organ and Reissner's fiber. In: Gross PM (ed) Circumventricular organs and body fluids, vol. II. CRC Press, Boca Raton, pp 3–41

Rodríguez S, Rodríguez PA, Banse C, Rodríguez EM, Oksche A (1987b) Reissner's fiber, massa caudalis and ampulla caudalis in the spinal cord of lamprey larvae (Geotria australis). Cell Tissue Res 247:359–366

Rodríguez EM, Hein S, Rodríguez S, Herrera H, Peruzzo B, Nualart F, Oksche A (1987c) Analysis of the secretory products of the subcommissural organ. In: Scharrer B, Korf HW, Hartwig HG (eds) Functional morphology of neuroendocrine systems. Springer, Berlin, pp 9–22

Rodríguez EM, Rodríguez S, Schoebitz K, Yulis CR, Hoffmann P, Manns V, Oksche A (1989) Light- and electron-microscopic investigation of the rat subcommissural organ grafted under the kidney capsule, with particular reference to immunocytochemistry and lectin histochemistry. Cell Tissue Res 258:499–514

Rodríguez S, Rodríguez EM, Jara P, Peruzzo B, Oksche A (1990) Single injection into the cerebrospinal fluid of antibodies against the secretory material of the subcommissural organ reversibly blocks formation of Reissner's fiber: immunocytochemical investigations in the rat. Exp Brain Res 81:113–124

Rodríguez EM, Oksche A, Hein S, Yulis CR (1992) Cell biology of the subcommissural organ. Int Rev Cytol 135:39–121

Rodríguez EM, del Brío León MA, Riera P, Menendez J, Schoebitz K (1996) The floor plate of the hindbrain is a highly specialized gland. Immunocytochemical and ultrastructural characteristics. Brain Res Dev Brain Res 97:153–168

Rodríguez EM, Rodríguez S, Hein S (1998) The subcommissural organ. Microsc Res Tech 41:98–123

Rodríguez S, Navarrete EH, Vío K, González C, Schöbitz K, Rodríguez EM (1999a) Isograft and xenograft of the subcommissural organ into the lateral ventricle of the rat and the formation of Reissner's fiber. Cell Tissue Res 296:457–469

Rodríguez S, Vio K, Wagner C, Barría M, Navarrete EH, Ramírez VD, Pérez-Fígares JM, Rodríguez EM (1999b) Changes in the cerebrospinal-fluid monoamines in rats with an immunoneutralization of the subcommissural organ-Reissner's fiber complex by maternal delivery of antibodies. Exp Brain Res 128: 278–290

Rodríguez EM, Oksche A, Montecinos H (2001) Human subcommissural organ, with particular emphasis on its secretory activity during the fetal life. Microsc Res Tech 52:573–590

Ruhaak LR, Hennig R, Huhn C, Borowiak M, Dolhain RJEM, Deelder AM, Rapp E, Wuhrer M (2010) Optimized workflow for preparation of APTS-labeled N-glycans allowing high-throughput analysis of human plasma glycomes using 48-channel multiplexed CGE-LIF. J Proteome Res 9:6655–6664

Sango K, Tokashiki A, Ajiki K, Horie M, Kawano H, Watabe K, Horie H, Kadoya T (2004) Synthesis, localization and externalization of galectin-1 in mature dorsal root ganglion neurons and Schwann cells. Eur J Neurosci 19:55–64

Schlattner U, Klaus A, Ramirez Rios S, Guzun R, Kay L, Tokarska-Schlattner M (2016) Cellular compartmentation of energy metabolism: creatine kinase microcompartments and recruitment of B-type creatine kinase to specific subcellular sites. Amino Acids 48:1751–1774

Schöbitz K, Garrido O, Heinrichs M, Speer L, Rodríguez EM (1986) Ontogenetical development of the chick and duck subcommissural organ. An immunocytochemical study. Histochemistry 84:31–41

Schöbitz K, Rodríguez EM, Garrido O, Del Brío León MA (1993) Ontogenetic development of the subcommissural organ with reference to the flexural organ. In: Oksche A, Rodríguez EM, Fernández-Llebrez P (eds) The Subcommissural Organ. Springer, Berlin Heidelberg New York, pp 41–49

Schöbitz K, González C, Peruzzo B, Yulis C, Rodríguez EM (2001) Organ culture of the bovine subcommissural organ. Evidence for synthesis and release of the secretory material. Microsc Res Tech 52:496–509

Stanka P, Schwink A, Wetzstein R (1964) Elektronenmikroskopische Untersuchungen des Subcommissuralorgans der Ratte. Z Zellforsch Mikrosk Anat 63:277–301

Sterba G (1962) Das Subcommissuralorgan von Lampetra planeri (Bloch). Zool Jahrb Anat 80:135–158

Sterba G (1964) Grundlage des histochemischen und biochemischen Nachweises von Neurosekret (Trägerprotein der Oxytocine) mit Pseudoisozyanin. Acta Histochem (Jena) 17:268–292

Sterba G (1966) Zur cerebrospinalen Neurokrinie der Wirbeltiere. Zool Anz Suppl 29:393–440

Sterba G (1969) Morphologie und Funktion des Subcommissuralorgans. In: Sterba G (ed) Zirkumventriculare Organe und Liquor. G Fischer, Jena, pp 17–27

Sterba G, Naumann W (1966) Elektronenmikroskopische Untersuchungen über den Reissnerschen Faden und die Ependymzellen im Rückenmark von *Lampetra planeri* (Bloch). Z Zellforsch Mikrosk Anat 72:516–524

Sterba G, Müller H, Naumann W (1967a) Fluoreszenz- und elektronenmikroskopische Untersuchungen über die Bildung des Reissnerschen Fadens bei *Lampetra Planeri* (Bloch). Z Zellforsch Mikrosk Anat 76:355–376

Sterba G, Ermisch A, Freyer K, Hartmann G (1967b) Incorporation of Sulphur-35 into the subcommissural organ and Reissner's fibre. Nature 216:504. https://doi.org/10.1038/216504a0

Sterba G, Wolf G, Scheuner G (1967c) Polarisatiosoptische Eigenschaften des Reissnerschen Fadens. Die Naturwissenschaften (18):495

Sterba G, KieBig C, Naumann W, Petter J, Kleim I (1982) The secretion of the subcommissural organ. A comparative immunocytochemical investigation. Cell Tissue Res 226:427–439

Sternberger LA, Hardy PH Jr, Cuculis JJ, Meyer HG (1970) The unlabeled antibody enzyme method of immunohistochemistry: preparation and properties of soluble antigen-antibody complex (horseradish peroxidase-antihorseradish peroxidase) and its use in identification of spirochetes. J Histochem Cytochem 18:315–333

Stowell SR, Arthur CM, Mehta P, Slanina KA, Blixt O, Leffler H, Smith DF, Cummings RD (2006) Galectin-1, -2, and -3 exhibit differential recognition of sialylated glycans and blood group antigens. J Biol Chem 283:10109–10123

Towbin H, Staehelin T, Gordon J (1979) Electrophoretic transfer of proteins from polyacrylamide gels to nitrocellulose sheets: procedure and some applications. Proc Natl Acad Sci U S A 76:4350–4354

Varki A, Cummings RD, Esko JD, Freeze HH, Stanley P, Marth JD, Bertozzi CR, Hart GW, Etzler ME (2009) Symbol nomenclature for glycan representation. Proteomics 9:5398–5399. https://doi.org/10.1002/pmic.200900708

Vío K, Rodríguez S, Navarrete EH, Pérez-Fígares JM, Jiménez AJ, Rodríguez EM (2000) Hydrocephalus induced by immunological blockage of the subcommissural organ-Reissner's fiber (RF) complex by maternal transfer of anti-RF antibodies. Exp Brain Res 135:41–52

Vío K, Rodríguez S, Yulis CR, Oliver C, Rodriguez EM (2008) The subcommissural organ of the rat secretes Reissner's fiber glycopro- teins and CSF-soluble proteins reaching the internal and external CSF compartments. Cerebr Fluid Res 5:1–14. https://doi.org/10.1186/1743-8454-5-3

Wagner C, Batiz LF, Rodríguez S, Jiménez AJ, Páez P, Tomé M, Pérez-Fígares JM, Rodríguez EM (2003) Cellular mechanisms involved in the stenosis and obliteration of the cerebral aqueduct of hyh mutant mice developing congenital hydrocephalus. J Neuropathol Exp Neurol 62:1019–1040

Wenger T, Klein MJ, Sorckel ME, Porte A, Stutinsky F (1969) Sur la structure fine de la fibre de Reissner et son mode de formation au niveau de l'organo sous-commissural chez le rat. Comp Rend Scienc Soc Biol 163:2436–2443

Wilson MR, Zoubeidi A (2016) BClusterin as a therapeutic target. Exp Opi Therap Targ. https://doi.org/10.1080/14728222.2017.1267142

Wolf G, Sterb G (1972) Zur stofflichen Charakteristik des Reissnerschen Fadens. Acta Zool (Stockh) 53:147–115

Yulis CR, Mota MD, Andrades JA, Rodríguez S, Peruzzo B, Mancera JM, Ramirez P, Garrido M, Pérez-Fígarez JM, Fernández-Llebrez P, Rodríguez EM (1998) Floor plate and the subcommissural organ are the source of secretory compounds of related nature: comparative immunocytochemical study. J Comp Neurol 392:19–34

Ziegels J (1976) The vertebrate subcommissural organ; a structural and functional review. Arch Biol 98:429–476